

1 Impact of Timanian thrust systems on the late 2 Neoproterozoic–Phanerozoic tectonic evolution of the 3 Barents Sea and Svalbard

4
5 Jean-Baptiste P. Koehl^{1,2,3,4}, Craig Magee⁵, Ingrid M. Anell⁶

6 ¹Centre for Earth Evolution and Dynamics (CEED), University of Oslo, PO Box 1028 Blindern, N-0315 Oslo,
7 Norway.

8 ²Department of Geosciences, UiT The Arctic University of Norway in Tromsø, N-9037 Tromsø, Norway.

9 ³Research Centre for Arctic Petroleum Exploration (ARCEX), UiT The Arctic University of Norway in Tromsø, N-
10 9037 Tromsø, Norway.

11 ⁴CAGE – Centre for Arctic Gas Hydrate, Environment and Climate, UiT The Arctic University of Norway in
12 Tromsø, N-9037 Tromsø, Norway.

13 ⁵School of Earth Science and Environment, University of Leeds, Leeds, LS2 9JT, United Kingdom.

14 ⁶Department of Geosciences, University of Oslo, P.O. Box 1047 Blindern, N-0316 Oslo, Norway.

15 **Correspondence:** Jean-Baptiste P. Koehl (jean-baptiste.koehl@uit.no)

16 17 **Abstract**

18 The Svalbard Archipelago consists of three basement terranes that record a complex
19 Neoproterozoic–Phanerozoic tectonic history, including four contractional events (Grenvillian,
20 Caledonian, Ellesmerian, and Eurekan) and two episodes of collapse- to rift-related extension
21 (Devonian–Carboniferous and late Cenozoic). Previous studies suggest these three terranes likely
22 accreted during the early–mid Paleozoic Caledonian and Ellesmerian orogenies. Yet recent
23 geochronological analyses show that the northwestern and southwestern terranes of Svalbard both
24 record an episode of amphibolite (–eclogite) facies metamorphism in the latest Neoproterozoic,
25 which may relate to the 650–550 Ma Timanian Orogeny identified in northwestern Russia, northern
26 Norway and the Russian Barents Sea. However, discrete Timanian structures have yet to be
27 identified in Svalbard and the Norwegian Barents Sea. Through analysis of seismic reflection, and
28 regional gravimetric and magnetic data, this study demonstrates the presence of continuous, several
29 kilometers thick, NNE-dipping, deeply buried thrust systems that extend thousands of kilometers
30 from northwestern Russia to northeastern Norway, the northern Norwegian Barents Sea, and the
31 Svalbard Archipelago. The consistency in orientation and geometry, and apparent linkage between

32 these thrust systems and those recognized as part of the Timanian Orogeny in northwestern Russia
33 and Novaya Zemlya suggests that the mapped structures are likely Timanian. If correct, these
34 findings would imply that Svalbard's three basement terranes and the Barents Sea were accreted
35 onto northern Norway during the Timanian Orogeny and should, hence, be attached to Baltica and
36 northwestern Russia in future Neoproterozoic–early Paleozoic plate tectonics reconstructions. In
37 the Phanerozoic, the study suggests that the interpreted Timanian thrust systems represented major
38 preexisting zones of weakness that were reactivated, folded, and overprinted by (i.e., controlled the
39 formation of new) brittle faults during later tectonic events. These faults are still active at present
40 and can be linked to folding and offset of the seafloor.

41

42 **Introduction**

43 Recognizing and linking tectonic events across different terranes is critical to plate
44 reconstructions. In the latest Neoproterozoic (at ca. 650–550 Ma), portions of northwestern Russia
45 (e.g., Timan Range and Novaya Zemlya) and the Russian Barents Sea were accreted to northern
46 Baltica by top-SSW thrusting during the Timanian Orogeny (Olovyanishnikov et al., 2000;
47 Kostyuchenko et al., 2006). Discrete Timanian structures with characteristic WNW–ESE strikes
48 are sub-orthogonal to the N–S-trending Caledonian grain formed during the closure of the Iapetus
49 Ocean (Gee et al., 1994; Witt-Nilsson et al., 1998; Johansson et al., 2004; 2005). Thus far,
50 Timanian structures have only been identified in onshore–nearshore areas of northwestern Russia
51 and northeastern Norway and offshore in the Russian Barents Sea and southeasternmost Norwegian
52 Barents Sea (Barrère et al., 2009, 2011; Marello et al., 2010; Gernigon et al., 2018; Hassaan et al.,
53 2020a, 2020b, [2021](#); [Hassaan, 2021](#)). Therefore, the nature of basement rocks in the northern and
54 southwestern Norwegian Barents Sea remains debatable. Some studies suggest a NE–SW-trending
55 Caledonian suture within the Barents Sea (Gudlaugsson et al., 1998; Gee and Teben'kov, 2004;
56 Breivik et al., 2005; Gee et al., 2008; Knudsen et al., 2019), whereas others argue for a swing into
57 a N–S trend and merging of Norway and Svalbard's Caledonides, which probably continue into
58 northern Greenland (Ziegler, 1988; Gernigon and Brönnner, 2012; Gernigon et al., 2014).
59 Regardless, these models solely relate basement structures in the northern and southwestern
60 Norwegian Barents Sea to the Caledonian Orogeny, implying that Laurentia and Svalbard were not
61 involved in the Timanian Orogeny and were separated from Baltica by the Iapetus Ocean in the

62 latest Neoproterozoic (Torsvik and Trench, 1991; Cawood et al., 2001; Cocks and Torsvik, 2005;
63 Torsvik et al., 2010; Merdith et al., 2021).

64 Nonetheless, geochronological data yielding Timanian ages suggest that deformation and
65 metamorphism contemporaneous of the Timanian Orogeny affected parts of the Svalbard
66 Archipelago and Laurentia and, possibly, all Arctic regions (Estrada et al., 2018; [Figure 1Figure](#)
67 [4a](#)): (1) eclogite facies metamorphism (620–540 Ma; Peucat et al., 1989; Dallmeyer et al., 1990b)
68 and eclogite facies xenoliths of mafic–intermediate granulite in Quaternary volcanic rocks are
69 found in northern Spitsbergen (648–556 Ma; Griffin et al., 2012); (2) amphibolite facies
70 metamorphism (643 ± 9 Ma; Majka et al., 2008, 2012, 2014; Mazur et al., 2009) and WNW–ESE-
71 striking shear zones like the Vimsodden–Kosibapasset Shear Zone (VKSZ; [Figure 1Figure 4b–c](#))
72 occur in southwestern Spitsbergen (600–537 Ma; Manecki et al., 1998; Faehnrich et al., 2020); and
73 (3) xenoliths of the subduction-related Midtkap igneous suite in northern Greenland yield Timanian
74 ages (628–570 Ma; Rosa et al., 2016; Estrada et al., 2018). In addition, several recent studies also
75 show the presence of NW–SE- to E–W-trending basement grain in the Norwegian Barents Sea,
76 which could possibly represent Timanian fabrics and structures ([Figure 1Figure 4b](#); Barrère et al.,
77 2009, 2011; Marelllo et al., 2010; Klitzke et al., 2019). Following these developments, a few paleo-
78 plate reconstructions now place Svalbard together with Baltica in the latest Neoproterozoic–
79 Paleozoic (e.g., Vernikovsky et al., 2011), and imply that the Norwegian Barents Sea and Svalbard
80 basement may contain Timanian structures overprinted during later (e.g., Caledonian) deformation
81 events.

82 To test the origin of basement grain in the northern Norwegian Barents Sea and Svalbard,
83 the present study focuses on several kilometers deep structures identified on 2D seismic reflection
84 data and correlated using regional gravimetric and magnetic data. These newly identified structures
85 trend WNW–ESE, i.e., parallel to the Timanian structural grain in northwestern Russia and
86 northern Norway ([Figure 1Figure 4a–c](#)). The structures are described and interpreted based on their
87 geometry and potential kinematic indicators, and are compared to well-known examples of
88 Caledonian and Timanian fabrics and structures elsewhere, e.g., onshore Norway (e.g., NNE-
89 dipping Trollfjorden–Komagelva Fault Zone – TKFZ; Siedlecka and Siedlecki, 1967; Siedlecka,
90 1975), in Svalbard (e.g., gently north-plunging Atomfjella Antiform – AA; Witt-Nilsson et al.,
91 1998), in northwestern Russia (NNE-dipping Central Timan Fault – CTF – [and related Mikulkin](#)
92 [Antiform](#); Siedlecka and Roberts, 1995; Olovyanishnikov et al., 2000; [Lorenz et al., 2004](#);

93 Kostyuchenko et al., 2006), and in the southern Norwegian Barents Sea (Barrère et al., 2011;
94 Gernigon et al., 2014) and the Russian Barents Sea (NNE-dipping Baidaratsky fault zone – BaFZ;
95 Lopatin et al., 2001; Korago et al., 2004; [Figure 1](#)~~Figure 1~~b–c). The present contribution proposes
96 a scenario involving several episodes of deformation starting in the Timanian Orogeny, and
97 involving reactivation and overprinting of Timanian structures during the Caledonian Orogeny,
98 Devonian–Carboniferous extension, Triassic extension, Eureka tectonism, and present-day
99 tectonism. Having established that Timanian structure may be present across the Barents Sea and
100 Svalbard, we briefly discuss the potential implications for the tectonic evolution of the Barents Sea
101 and the Svalbard Archipelago and associated basins (e.g., Ora and Olga basins; Anell et al., 2016).

102 Should our interpretation of discrete Timanian structures throughout the Norwegian
103 Barents Sea and Svalbard be validated by future research, it would support accretion of these
104 terranes to Baltica in the late Neoproterozoic and place the Caledonian suture farther west than is
105 commonly suggested (e.g., Breivik et al., 2005; Gernigon et al., 2014), thus leading to a major
106 revision of plate tectonics models. In addition, constraining the extent and reactivation history of
107 such faults may shed some light on their influence on younger tectonic events, such as Caledonian,
108 Ellesmerian and Eureka contraction, Devonian–Carboniferous collapse–rifting, and late Cenozoic
109 breakup and ongoing extension.

110

111 **Geological setting**

112 *Timanian Orogeny*

113 The Timanian Orogeny corresponds to a ca. 650–550 Ma episode of NNE–SSW
114 contractional deformation that affected northwestern Russia and northeastern Norway. During this
115 tectonic episode, crustal-scale, WNW–ESE-striking, NNE-dipping thrusts systems with south-
116 southwestwards transport direction (top-SSW; Siedlecka and Siedlecki, 1967; Siedlecka, 1975;
117 [Figure 1](#)~~Figure 1~~b), accreted portions of the Russian Barents Sea and northwestern Russia onto
118 northeastern Baltica, including Novaya Zemlya, Severnaya Zemlya, the Kanin Peninsula, the
119 Timan Range, and the Kola Peninsula (Siedlecka and Roberts, 1995; Olovyanishshnikov et al.,
120 2000; Roberts and Siedlecka, 2002; Gee and Pease, 2004; Kostyuchenko et al., 2006; Lorenz et al.,
121 2008; Marelli et al., 2013) and the Varanger Peninsula in northeastern Norway (Siedlecka and
122 Siedlecki, 1967; Siedlecka, 1975; Roberts and Olovyanishshnikov, 2004; Herrevold et al., 2009;
123 Drachev, 2016; [Figure 1](#)~~Figure 1~~a). Major Timanian thrusts include the NNE-dipping Baidaratsky

124 fault zone in the Russian Barents Sea and Novaya Zemlya (~~Figure 1~~Figure 1a–b; Eldholm and
125 Ewing, 1971, their figure 4 profile C–D; Lopatin et al., 2001; Korago et al., 2004; Drachev, 2016),
126 the NNE-dipping Central Timan Fault (and associated thrust anticline, the Mikulkin Antiform) on
127 the Kanin Peninsula and the Timan Range (Siedlecka and Roberts, 1995; Olovyanishnikov et al.,
128 2000; Lorenz et al., 2004; Kostyuchenko et al., 2006), and the NNE-dipping Trollfjorden–
129 Komagelva Fault Zone in northern Norway (Siedlecka and Siedlecki, 1967; Siedlecka, 1975;
130 Herrevold et al., 2009).

131

132 *Accretion of Svalbard basement terranes in the early Paleozoic*

133 The Svalbard Archipelago consists of three Precambrian basement terranes (Figure 2),
134 some of which show affinities with Greenland (northwestern and northeastern terranes), whereas
135 others are possibly derived from Pearya (southwestern terrane; Harland and Wright, 1979; Ohta et
136 al., 1989; Gee and Teben'kov, 2004; Labrousse et al., 2004; Piepjohn et al., 2013; Fortey and
137 Bruton, 2013). These terranes possibly accreted during the mid-Paleozoic Caledonian (collision of
138 Greenland with Svalbard and Norway at ca. 460–410 Ma; Horsfield, 1972; Dallmeyer et al., 1990a;
139 Johansson et al., 2004, 2005; Faehnrich et al., 2020) and Late Devonian Ellesmerian orogenies
140 (Piepjohn, 2000; Majka and Kosminska, 2017). In these models, accretion was facilitated via
141 hundreds of kilometers of displacement along (arcuate) N–S-striking strike-slip faults, such as the
142 Billefjorden Fault Zone (BFZ – Harland, 1969; Harland et al., 1992; Labrousse et al., 2008) and
143 the Lomfjorden Fault Zone (LFZ – Piepjohn et al., 2019; Figure 2Figure 2), although other studies
144 suggest more limited strike-slip displacement (Lamar et al., 1986; Manby and Lyberis, 1992;
145 Manby et al., 1994; Lamar and Douglass, 1995). Some previous workers assumed that these large
146 (strike-slip?) faults extended thousands of kilometers southwards and represented the continuation
147 of Caledonian faults in Scotland (Norton et al., 1987; Dewey and Strachan, 2003). Caledonian
148 contraction resulted in the formation of large fold and thrust complexes, such as the N–S-trending,
149 gently north-plunging Atomfjella Antiform in northeastern Spitsbergen (Gee et al., 1994; Witt-
150 Nilsson et al., 1998) and the N–S-trending Rijpdalen Anticline in Nordaustlandet (Johansson et al.,
151 2004; 2005; Dumais and Brönnner, 2020), whereas Ellesmerian tectonism may have formed narrow
152 N–S-trending fold and thrust belts, like the Dickson Land and Germaniahelvøya fold-thrust zones
153 (McCann, 2000; Piepjohn, 2000; Dallmann and Piepjohn, 2020).

154 In northern Norway, Timanian thrusts were reactivated–overprinted in subsequent tectonic
155 events (e.g., Caledonian Orogeny and late–post-Caledonian collapse–rifting) as dominantly strike-
156 to oblique-slip faults (Siedlecka and Siedlecki, 1971; Roberts et al., 1991; Herrevold et al., 2009;
157 Rice, 2014). A notable example is the folding and reactivation of Timanian fabrics and structures
158 (e.g., NNE-dipping Trollfjorden–Komagelva Fault Zone) during the Caledonian Orogeny
159 (Siedlecka and Siedlecki, 1971; Herrevold et al., 2009) and intrusion of Mississippian dolerite
160 dykes along steeply dipping WNW–ESE-striking brittle faults that overprint the Trollfjorden–
161 Komagelva Fault Zone onshore–nearshore northern Norway (Roberts et al., 1991; Lippard and
162 Prestvik, 1997; Nasuti et al., 2015; Koehl et al., 2019).

163

164 *Late Paleozoic post-Caledonian collapse and rifting*

165 In the latest Silurian–Devonian, extensional collapse of the Caledonides led to the
166 deposition of several kilometers thick sedimentary basins such as the Devonian Graben in northern
167 Spitsbergen (Gee and Moody-Stuart, 1966; Friend et al., 1966; Friend and Moody-Stuart, 1972;
168 Murascov and Mokin, 1979; Manby and Lyberis, 1992; Manby et al., 1994; Friend et al., 1997;
169 McCann, 2000; Dallmann and Piepjohn, 2020). In places, N–S-trending basement ridges
170 potentially exhumed as metamorphic core complexes along bowed, reactivated detachments, such
171 as the Keisarhjelmen Detachment in northwestern Spitsbergen (Braathen et al., 2018).

172 In the latest Devonian–Mississippian, coal-rich sedimentary strata of the Billefjorden
173 Group were deposited within normal fault-bounded basins throughout Spitsbergen (Cutbill and
174 Challinor, 1965; Harland et al., 1974; Cutbill et al., 1976; Aakvik, 1981; Koehl and Muñoz-Barrera,
175 2018; Koehl, 2020a) and the Norwegian Barents Sea (Koehl et al., 2018a; Tonstad, 2018). As rift-
176 related normal faulting evolved, Pennsylvanian sedimentation was localized into a few, several
177 kilometers deep, N–S-trending basins like the Billefjorden Trough (Cutbill and Challinor, 1965;
178 Braathen et al., 2011; Koehl et al., 2021 in review) and the E–W-trending Ora Basin (Anell et al.,
179 2016). In the Permian, rift-related faulting stopped and platform carbonates were deposited
180 throughout Svalbard (Cutbill and Challinor, 1965) and the Barents Sea (Larssen et al., 2005).

181 Overall, the several kilometers thick, late Paleozoic sedimentary succession deposited
182 during late–post-Caledonian extension buried Proterozoic basement rocks. As a result, these rocks
183 are sparsely exposed and, thus, difficult to study.

184

185 ***Mesozoic sedimentation and magmatism***

186 In the Mesozoic, Svalbard and the Barents Sea remained tectonically quiet and were only
187 affected by minor Triassic normal faulting (e.g., Anell et al., 2013; Osmundsen et al., 2014; Ogata
188 et al., 2018; Smyrak-Sikora et al., 2020). In the Early Cretaceous, Svalbard was affected by a
189 regional episode of magmatism recorded by the intrusion of numerous dykes and sills of the
190 Diabasodden Suite (Senger et al., 2013).

191

192 ***Early Cenozoic Eureka tectonism***

193 The opening of the Labrador Sea and Baffin Bay between Greenland and Arctic Canada in
194 the early Cenozoic (Chalmers and Pulvercraft, 2001; Oakey and Chalmers, 2012) led to the
195 collision of northern Greenland with Svalbard and the formation of a fold-and-thrust belt with top-
196 east thrusts and east-verging folds in western Spitsbergen (Dallmann et al., 1993). In eastern
197 Spitsbergen, this deformation event is characterized by dominantly thin-skinned deformation
198 structures, including décollements, some of which showing westwards transport directions
199 (Andresen et al., 1992; Haremo and Andresen, 1992). Notably, the N–S-striking Agardhbukta
200 Fault, a major splay/segment of the N–S-striking Lomfjorden Fault Zone, accommodated reverse
201 and, possibly, strike-slip movements during this event (Piepjohn et al., 2019).

202

203 ***Late Cenozoic opening of the Fram Strait***

204 After the end of extension in the Labrador Sea and Baffin Bay, the Fram Strait started to
205 open in the earliest Oligocene (Engen et al., 2008). Tectonic extension and break-up in the Fram
206 Strait resulted in the formation of two major, NW–SE-striking transform faults (Lowell, 1972;
207 Thiede et al., 1990; [Figure 1](#)~~Figure 1b~~).

208

209 **Methods and datasets**

210 Seismic surveys from the DISKOS database (see [Figure 1](#)~~Figure 1b–c~~ and supplement S1
211 for location) were used to interpret basement-seated structures and related, younger, brittle
212 overprints ([Figure 3](#)~~Figure 3a–f~~ and [Figure 4](#)~~Figure 4a–h~~ and supplement S2). Other features of
213 interest include potential dykes, which commonly appear as high positive reflections on seismic
214 data. The geology interpreted from onshore seismic data was directly correlated to geological maps
215 of the Norwegian Polar Institute (e.g., Dallmann, 2015). Where possible, interpretation of offshore

216 seismic data was tied to onshore geological maps and to exploration wells Raddedalen-1 and
217 Plurdalen-1 on Edgeøya (Bro and Shvarts, 1983; Harland and Kelly, 1997) and to the Hopen-2 well
218 on Hopen (Anell et al., 2014; ~~Figure 1~~Figure 1c and supplement S3). The Raddedalen-1 well
219 penetrated 2823 meters of Upper Permian to Mississippian or Ordovician strata, the Plurdalen well
220 2351 meters of Middle Triassic to (pre-?) Devonian strata, and the Hopen-2 well 2840 meters of
221 Middle–Upper Triassic to Pennsylvanian strata (Bro and Shvarts, 1983; Harland and Kelly, 1997;
222 Anell et al., 2014; Senger et al., 2019). Note that the present contribution favors interpretation of
223 lower Paleozoic (Ordovician–Silurian) rocks in the Raddedalen-1 well by Bro and Shvarts (1983)
224 to that of upper Paleozoic (Upper Devonian–Mississippian) by Cambridge Svalbard Exploration
225 (see contrasting interpretations in Harland and Kelly, 1997). This is based on the more detailed
226 lithological, palynological and paleontological analyses by the former, and on the strong contrast
227 of the lithologies described in the well with Devonian–Mississippian successions on Svalbard
228 (Cutbill and Challinor, 1965; Cutbill et al., 1976; Friend et al., 1997; Dallmann and Piepjohn,
229 2020).

230 The present contribution only includes a few examples of seismic sections. However, more
231 interpreted and uninterpreted seismic data are available as supplements (supplements S1–2) and
232 from the Norwegian Petroleum Directorate (DISKOS database). None of the seismic sections were
233 depth-converted, and thicknesses therefore appear in seconds (Two-Way Time; TWT). However,
234 local time conversion was performed to tie seismic wells onshore Edgeøya to seismic section in
235 Storfjorden and depth conversion was performed locally to evaluate fault displacement. Velocities
236 of Gernigon et al. (2018) were used in these conversions. -Supplement S3 includes further details
237 related to these conversions.

238 The boundary between Precambrian, lower Paleozoic and upper Paleozoic successions
239 offshore are interpreted as major unconformities that truncate underlying reflections and fold
240 structures (e.g., Figure 3a, b and c). The boundaries between Devonian–Permian and Mesozoic
241 successions were tied to the Raddedalen-1, Plurdalen-1, and Hopen-2 exploration wells for offshore
242 parts of the study area. The boundary between Devonian–Mississippian and Pennsylvanian–
243 Permian onshore Svalbard are interpreted as a major unconformity truncating Devonian–
244 Mississippian dykes (see Figure 3e).

245 The correlation of kilometer-thick structures discussed in the present contribution was also
246 tested using gravimetric and magnetic data in cross section (~~Figure 3~~Figure 3a–f) and regional

247 magnetic and gravimetric data in the northern Norwegian Barents Sea and Svalbard ([Figure](#)
248 [5Figure-5](#) and supplement S4) from the Federal Institute for Geosciences and Natural Resources in
249 Germany in map view (Klitzke et al., 2019). Regional gravimetric and magnetic data are also used
250 to interpret deep basement fabrics and structures, e.g., regional folds (gravimetric highs commonly
251 associated with major anticlines of thickened dense basement [with high metamorphic grade](#) (i.e.,
252 Precambrian) rocks [\(e.g., Mikulkin Antiform; Lorenz et al., 2004; Kostyuchenko et al., 2006\)](#) and
253 gravimetric lows with synclines with less dense sedimentary basins) and large faults [bounding](#)
254 [magmatic complexes and/or intruded by magmatic bodies](#) that commonly correlate with elongated
255 gravimetric and/or magnetic anomalies (e.g., [Kostyuchenko et al., 2006; Koehl et al., 2019](#)), and
256 to discuss the relationship of the described structures with known structural trends in onshore
257 basement rocks in Russia, Norway and Svalbard. [Magnetic and gravimetric anomalies not related](#)
258 [to Timanian and Caledonian grains will not be discussed in the present study.](#)

259

260 **Results and interpretations**

261 First, the interpretation of seismic data are described by area, including (1) Storfjorden
262 (between Edgeøya and Spitsbergen) and the northeastern part of the Norwegian Barents Sea (east
263 of Edgeøya), (2) Nordmannsfonna to Sassenfjorden onshore–nearshore the eastern–central part of
264 Spitsbergen, and (3) the northwestern part of the Norwegian Barents Sea between Bjørnøya and
265 Spitsbergen ([Figure 1Figure-1](#)b–c). Description in each area starts with deep Precambrian basement
266 rocks and shallow sedimentary rock units, and ends with deep brittle–ductile structures and with
267 shallow brittle faults. Then, potential field data and regional gravimetric and magnetic anomalies
268 in the Barents Sea and Svalbard are described, and compared and correlated to seismic data and to
269 major Timanian and Caledonian fabrics and structures onshore northwestern Russia, Svalbard and
270 Norway. Please see high resolution versions of all the figures and supplements on DataverseNO
271 (doi.org/10.18710/CE8RQH).

272

273 *Structures in the northwestern–northeastern Norwegian Barents Sea, Storfjorden and central–* 274 *eastern Spitsbergen*

275 *Storfjorden and northeastern Norwegian Barents Sea*

276 Folded Precambrian–lower Paleozoic basement rocks

277 Seismic facies at depths of 2–6 seconds (TWT) typically comprise successions of laterally
278 discontinuous (< three kilometers long), sub-horizontal, moderately curving–undulating,
279 moderate–high-amplitude seismic reflections that alternate with packages of highly-disrupted
280 and/or curved low-amplitude seismic reflections (see yellow lines within pink and purple units in
281 [Figure 3Figure 3a](#) and [Figure 4Figure 4a](#)). The curving geometries of the moderate–high amplitude
282 reflections display a typical kilometer- to hundreds of meter-scale wavelength and are commonly
283 asymmetric, seemingly leaning/verging towards the south/SSW (see yellow lines in [Figure 4Figure](#)
284 [4b](#)). Based on ties with well bores on Edgeøya (Raddedalen-1 well; Bro and Shvarts, 1983; Harland
285 and Kelly, 1997), these asymmetric, undulate features most likely correspond to SSW-verging
286 folds in Precambrian–lower Paleozoic basement rocks. In places, apparent reverse offsets of these
287 undulate reflections align along moderately–gently north- to NNE-dipping surfaces (see red lines
288 in [Figure 4Figure 4a](#) and c), which are therefore interpreted as minor, top-south/SSW, brittle
289 thrusts.

290 Upper Paleozoic–Mesozoic sedimentary successions

291 In Storfjorden and the northwestern Norwegian Barents Sea, shallow (0–3 seconds TWT)
292 seismic reflections above folded and thrust Precambrian–lower Paleozoic basement rocks show
293 significantly more continuous patterns (>> five kilometers), gently curving–undulating geometries
294 and only local disruptions by shallow, dominantly NNE-dipping, high-angle listric disruptions (see
295 yellow lines within orange unit in [Figure 3Figure 3a](#) and c). In the northeastern Barents Sea, these
296 reflections are largely flat-lying (see yellow lines within orange unit in [Figure 3Figure 3b](#) and d).
297 Based on field mapping campaigns and well-bores in adjacent onshore areas of Spitsbergen,
298 Edgeøya, Hopen and Bjørnøya (see location in [Figure 1Figure 1b](#)), these continuous reflections are
299 interpreted as mildly folded upper Paleozoic–Mesozoic (–Cenozoic?) sedimentary strata
300 (Dallmann and Krasil’scikov, 1996; Harland and Kelly, 1997; Worsley et al., 2001; Dallmann,
301 2015). The Permian–Triassic boundary was correlated throughout the northern Norwegian Barents
302 Sea and Storfjorden by using the tie of Anell et al. (2014) to the Hopen-2 well.

303 Deep thrust systems

304 The packages of sub-horizontal, moderately curving–undulating (folded Precambrian–
305 lower Paleozoic basement) reflections alternate laterally from north to south with 20–60 kilometers
306 wide, up to four seconds thick (TWT), upwards-thickening, wedge-shaped packages (areas with
307 high concentrations of black lines in [Figure 3Figure 3a](#) and d). These wide upwards-thickening

308 packages consist of two types of reflections. First, they include planar, continuous, gently-
309 moderately north- to NNE-dipping, sub-parallel, high-amplitude reflections that commonly merge
310 together downwards and that can be traced and correlated on several seismic sections in Storfjorden
311 (black lines in [Figure 3Figure-3a](#)). Upwards, these reflections terminate against high-amplitude
312 convex-upwards reflections interpreted as intra- Precambrian-lower Paleozoic basement
313 reflections (fuchsia lines in [Figure 3Figure-3a](#) and c) or continue as moderately NNE-dipping
314 disruption surfaces that offset these intra-basement reflections top-SSW (e.g., offset intra-
315 Precambrian unconformities in [Figure 3Figure-3a](#) and c and [Figure 4Figure-4d](#)).

316 Second, sub-parallel, high-amplitude reflections bound wedge-shaped, upwards-thickening
317 packages of asymmetric, curved, south- to SSW-leaning, moderately north- to NNE-dipping,
318 moderate-amplitude reflections showing narrow (< one kilometer wide) upwards-convex
319 geometries ([Figure 4Figure-4d](#)). These asymmetric reflections also commonly appear as gently
320 north- to NNE-dipping packages of Z-shaped reflections bounded by sub-parallel, planar, high-
321 amplitude reflections (see yellow lines in [Figure 4Figure-4e](#)). Asymmetric, south- to SSW-leaning,
322 convex-upwards reflections are interpreted as south- to SSW-verging fold anticlines reflecting
323 relatively low amounts of plastic deformation of layered rocks.

324 The alternation of packages of layered rocks folded into SSW-verging folds (yellow lines
325 in [Figure 3Figure-3a-c](#)) with packages of planar, NNE-dipping, sub-parallel, high-amplitude
326 reflections (black lines in [Figure 3Figure-3a-c](#)) suggest that the latter reflection packages represent
327 zones where initial layering was destroyed and/or possibly reoriented, i.e., areas that
328 accommodated larger amounts of deformation and tectonic displacement. Thus, planar, gently-
329 moderately north- to NNE-dipping, high-amplitude reflections (black lines in [Figure 3Figure-3a-](#)
330 c) are interpreted as low-angle brittle-ductile thrust systems. We name these thrust systems (from
331 north to south) the Steiløya-Krylen (SKFZ), Kongsfjorden-Cowanodden (KCFZ),
332 Bellsundbanken (BeFZ), and Kinnhøgda-Daubjørnpynten fault zones (KDFZ; [Figure 3Figure-3a](#)
333 and supplement S2a-b; see [Figure 1Figure-1c](#) for location of the thrusts).

334 The relatively high-amplitude character of planar, NNE-dipping reflections within the
335 thrusts suggest that these tectonic structures consist of sub-parallel layers of rocks and minerals
336 with significantly different physical properties. A probable explanation for such laterally
337 continuous and consistently high-amplitude reflections is partial recrystallization of rocks layers-
338 mineral bands into rocks and minerals with significantly higher density along intra-thrust planes

339 that accommodated large amounts of displacement (e.g., mylonitization; Fountain et al., 1984;
340 Hurich et al., 1985). In places, packages of aggregates of Z-shaped reflections bounded upwards
341 and downwards by individual low-angle thrust surfaces are interpreted as forward-dipping duplex
342 structures (e.g., Boyer and Elliott, 1982) reflecting relatively strong plastic deformation between
343 low-angle, brittle–ductile (mylonitic?) thrusts (see yellow lines in [Figure 4](#)[Figure 4e](#)).

344 The Kongsfjorden–Cowanodden, Bellsundbanken, and Kinnhøgda–Daudbjørnpynten fault
345 zones can be traced east-southeast of Edgeøya as a similar series of 20–60 kilometers wide, up to
346 four seconds thick (TWT), upwards-thickening packages (e.g., black lines in [Figure 3](#)[Figure 3d](#)
347 and supplements S2a). However, their imaging along NNW–SSE-trending seismic sections is
348 much more chaotic and it is more difficult to identify smaller structures (like south-verging folds
349 and minor thrusts) within each thrust system (e.g., supplement S2a). This suggests that these three
350 thrust systems strike oblique to NNW–SSE-trending seismic sections (supplement S2a), whereas
351 they are most likely sub-orthogonal to N–S- to NNE–SSW-trending seismic sections in Storfjorden
352 ([Figure 3](#)[Figure 3a](#)). The only orientation that reconciles these seismic facies variations (i.e., well-
353 imaged on NNE–SSW-trending seismic sections and poorly imaged by NNW–SSE-trending
354 seismic sections; [Figure 3](#)[Figure 3a](#) and supplement S2a) is an overall WNW–ESE strike.

355 South of each 20–60 kilometers wide packages of thrust surfaces and related fold and
356 duplex structures, seismic reflections representing Precambrian–lower Paleozoic basement rocks
357 typically appear as gently curved, convex-upwards, relatively continuous reflections showing sub-
358 horizontal seismic onlaps (see white arrows in [Figure 3](#)[Figure 3a–f](#)). This suggests that
359 Precambrian–lower Paleozoic basement rocks most likely consist (meta-) sedimentary rocks
360 (analogous to those observed in northeastern Spitsbergen and Nordaustlandet; Harland et al., 1993;
361 Stouge et al., 2011) that were deposited in foreland and piggy-back basins ahead of each 20–60
362 kilometers wide packages ([Figure 3](#)[Figure 3a–f](#)).

363 Hence, based on the upwards-thickening geometry of the packages of south- to SSW-
364 verging folds and of forward-dipping duplexes, on the top-SSW reverse offsets of intra-basement
365 reflections by low-angle brittle–ductile thrust surfaces, on the upwards truncation of these low-
366 angle thrusts by intra-basement reflections, and on the overlapping geometries of (meta-)
367 sedimentary basement rocks south of each set of top-SSW thrust surfaces, the 20–60 kilometers
368 wide, upwards-thickening, wedge-shaped packages are interpreted as crustal-scale, several
369 kilometers thick, north- to NNE-dipping, top-SSW, brittle–ductile thrust systems (see fault zones

370 with high concentration of black lines in [Figure 3](#)~~Figure 3~~a–f). These thrust systems include low-
371 angle, brittle–ductile, mylonitic thrust surfaces (black lines in [Figure 4](#)~~Figure 4~~d–e) separating
372 upwards-thickening thrust sheets that consist of gently to strongly folded basement rocks and
373 forward-dipping duplex structures (yellow lines in [Figure 4](#)~~Figure 4~~d–e). These thrust sheets are
374 interpreted to reflect accretion and stacking from the north or north-northeast. The interpreted thrust
375 systems are comparable in seismic facies and thickness to kilometer-thick mylonitic shear zones in
376 the Norwegian North Sea (Phillips et al. 2016) and southwestern Norwegian Barents Sea (Koehl et
377 al., 2018).

378 N–S-trending folds

379 On E–W seismic cross sections, reflections of the Kongsfjorden–Cowanodden,
380 Bellsundbanken, and Kinnhøgda–Daudbjørnpynten fault zones define large, 50–100 kilometers
381 wide, U-shaped, symmetrical depressions (black lines in [Figure 3](#)~~Figure 3~~b) on the edge of which
382 they are truncated at a high angle and overlain by folded lower Paleozoic and mildly folded to flat-
383 lying upper Paleozoic (meta-) sedimentary rocks (purple and orange units with associated yellow
384 lines in [Figure 3](#)~~Figure 3~~b). In addition, within these U-shaped depressions, the thrust systems show
385 curving up and down, symmetrical geometries with 5–15 kilometers wavelength (yellow lines
386 within the pink unit in [Figure 3](#)~~Figure 3~~b and [Figure 4](#)~~Figure 4~~f). Also notice the kilometer- to
387 hundreds of meter-scale undulating pattern of 5–15 kilometers wide curved geometries (yellow
388 lines in [Figure 4](#)~~Figure 4~~f). Based on the truncation and abrupt upward disappearance of high-
389 amplitude seismic reflections characterizing the thrust systems, the high-angle truncation of the
390 thrusts is interpreted as a major erosional unconformity (dark blue line in [Figure 3](#)~~Figure 3~~b and
391 pink line in [Figure 4](#)~~Figure 4~~f), and the large U-shaped depressions as large N–S- to NNE–SSW-
392 trending, upright regional folds (black lines in [Figure 3](#)~~Figure 3~~b). Furthermore, the 5–15
393 kilometers wide, symmetrical, curved geometries and associated, kilometer- to hundreds of meter-
394 scale, undulating pattern of seismic reflections within the thrusts are interpreted as similarly (N–S-
395 to NNE–SSW-) trending, upright, parasitic macro- to meso-scale folds (yellow lines in [Figure](#)
396 [3](#)~~Figure 3~~b and [Figure 4](#)~~Figure 4~~f).

397 Shallow brittle faults

398 In places, near the top of the 20–60 kilometers wide thrust systems (Kongsfjorden–
399 Cowanodden, Bellsundbanken, and Kinnhøgda–Daudbjørnpynten fault zones), low-angle brittle–
400 ductile thrust surfaces merge upwards with high-angle to vertical, listric, north- to NNE-dipping

401 disruption surfaces at depths of c. 2–3 seconds (TWT; see red lines in [Figure 3](#)~~Figure 3~~a and d).
402 These listric disruption surfaces truncate shallow, laterally continuous reflections that display
403 gently curved, symmetric geometries in Storfjorden (yellow lines in [Figure 3](#)~~Figure 3~~a) and flat-
404 lying geometries in the northeastern Norwegian Barents Sea (yellow lines in [Figure 3](#)~~Figure 3~~d).
405 Notably, they show minor, down-NNE normal offsets, and related minor southwards thickening
406 (towards the disruption) of seismic sub-units within Devonian–Carboniferous (–Permian?)
407 sedimentary strata in the north, both in Storfjorden and the northeastern Barents Sea ([Figure](#)
408 [3](#)~~Figure 3~~a–d and white double arrows in [Figure 4](#)~~Figure 4~~g). In addition, they display minor
409 reverse offsets and associated gentle upright folding of shallow continuous reflections potentially
410 representing upper Mesozoic (–Cenozoic?) sedimentary deposits in Storfjorden ([Figure 3](#)~~Figure~~
411 [3](#)~~Figure 3~~a–c and e, and orange lines in [Figure 4](#)~~Figure 4~~h). Note that flat-lying Mesozoic (–Cenozoic?)
412 sedimentary rocks are not offset in the northeastern Norwegian Barents Sea ([Figure 3](#)~~Figure 3~~d).

413 Based on the observed normal offsets and southwards-thickening of Devonian–
414 Carboniferous (–Permian?) sedimentary strata north of these disruption surfaces (e.g., white double
415 arrows in [Figure 4](#)~~Figure 4~~g), these are interpreted as syn-sedimentary Devonian–Carboniferous
416 normal faults. The minor reverse offsets and associated gentle upright folding of Mesozoic (–
417 Cenozoic?) sedimentary rocks in Storfjorden (e.g., orange lines in [Figure 4](#)~~Figure 4~~h) suggest that
418 these normal faults were mildly inverted near Svalbard in the Cenozoic. However, it is unclear
419 whether inversion in Storfjorden initiated in the early Cenozoic or later. Nonetheless, minor reverse
420 offset and folding of the seafloor clearly indicate ongoing inversion along these faults ([Figure](#)
421 [3](#)~~Figure 3~~a and c, and [Figure 4](#)~~Figure 4~~h). Furthermore, considering the merging relationship
422 between these high-angle listric disruption surfaces and underlying shear zones (i.e., merging black
423 and red lines in [Figure 3](#)~~Figure 3~~a and c–d), we propose that the formation of Devonian–
424 Carboniferous normal faults was controlled by the crustal-scale, north- to NNE-dipping (inherited)
425 thrust systems (Kongsfjorden–Cowanodden, Bellsundbanken, and Kinnhøgda–Daudbjørnpynten
426 fault zones).

427

428 *Nordmannsfonna–Sassenfjorden (eastern–central Spitsbergen)*

429 Deep thrust system and N–S-trending folds

430 Seismic data from Nordmannsfonna to Sassenfjorden in eastern Spitsbergen (see [Figure](#)
431 [1](#)~~Figure 1~~c for location) show reflection packages including both planar, continuous, moderately-

432 dipping high-amplitude reflections and upwards-curving, moderate-amplitude reflections (black
433 and yellow lines in [Figure 3](#)[Figure 3e–f](#)). These two sets are similar to reflection packages
434 interpreted as low-angle, brittle–ductile mylonitic thrusts bounding packages of south- to SSW-
435 verging folds in Storfjorden and the northeastern Norwegian Barents Sea (black and yellow lines
436 in [Figure 3](#)[Figure 3a](#) and [d](#), and supplement S2a). In addition, they are located at similar depths (>
437 2 seconds TWT) and seem to align with the Kongsfjorden–Cowanodden fault zone in Storfjorden
438 along a WNW–ESE-trending axis. Hence, we interpret the deep, continuous, high-amplitude
439 reflections in eastern Spitsbergen as the western continuation of the top-SSW Kongsfjorden–
440 Cowanodden fault zone. This thrust can be traced on seismic data as gently NNE-dipping, high-
441 amplitude reflections in Sassendalen and Sassenfjorden–Tempelfjorden (supplement S2c–d), and
442 possibly in Billefjorden (Koehl et al., 2021 in review, their figure 9a–b).

443 In Nordmannsfonna, the base-Pennsylvanian unconformity (white line in [Figure 3](#)[Figure](#)
444 [3e–f](#); tied to onshore geological maps; Dallmann, 2015) truncates the Kongsfjorden–Cowanodden
445 fault zone (black lines in [Figure 3](#)[Figure 3e–f](#)) upwards and the fault shows pronounced variations
446 in dip direction, ranging from east-dipping in the east to NNE-dipping in the north and WNW-
447 dipping in the west, which result into a c. 15–20 kilometers wide, north- to NNE-plunging dome-
448 shaped/convex-upwards geometry (black lines in [Figure 3](#)[Figure 3e–f](#)). This portion of the thrust
449 system is interpreted to be folded into a major NNE- to north-plunging upright fold, whose 3D
450 geometry was accurately constrained due to good seismic coverage in this area ([Figure 1](#)[Figure](#)
451 [1c](#)).

452 Small-scale structures within the Kongsfjorden–Cowanodden fault zone also show
453 asymmetric folds and internal seismic units terminating upwards with convex-upwards reflections
454 (yellow lines in [Figure 3](#)[Figure 3e–f](#)) suggesting top-SSW nappe thrusting in the northern portion
455 of the thrust system. However, on E–W cross sections, seismic data reveal a set of west-verging
456 folds in the east and a more chaotic pattern of symmetrical, dominantly upright folds in the west
457 (yellow lines in [Figure 3](#)[Figure 3e](#)) and below a major, high-angle, east-dipping disruption surface
458 (thick red line in [Figure 3](#)[Figure 3e](#)) that crosscuts the Kongsfjorden–Cowanodden fault zone.

459 Shallow brittle faults

460 The high-angle, east-dipping disruption surface (thick red line in [Figure 3](#)[Figure 3e](#)) is
461 associated with minor subvertical to steeply east-dipping disruption surfaces (thin red lines in
462 [Figure 3](#)[Figure 3e](#)). This feature shows a major reverse, top-west offset (> 0.5 second TWT) of

463 seismic units and reflections at depth > 0.75 second (TWT; e.g., black lines in [Figure 3Figure 3e](#)),
464 and minor reverse offset (< 0.1 second TWT) and upwards-convex curving of adjacent reflections
465 at depth < 0.75 second (TWT; white line and yellow lines within blue and units in [Figure 3Figure](#)
466 [3e](#)). Since the major disruption coincides with the location of the Agardhbukta Fault (Piepjohn et
467 al., 2019; see [Figure 1Figure 1](#) for location) and shows a steep inclination near the surface similar
468 to that of the Agardhbukta Fault, it is interpreted as the subsurface expression of this fault. The
469 Agardhbukta Fault offsets the Kongsfjorden–Cowanodden fault zone in a reverse fashion (>0.5
470 second TWT; black lines in [Figure 3Figure 3e](#)), and terminates upwards within and slightly offsets
471 upper Paleozoic–Mesozoic sedimentary rocks (blue and black units and associated yellow lines in
472 [Figure 3Figure 3e](#)), which were correlated to onshore outcrops in eastern Spitsbergen (Andresen et
473 al., 1992; Haremo and Andresen, 1992; Dallmann, 2015). As a result, these rocks are folded into a
474 N–S-trending, open, upright fold around the fault tip, both of which suggest top-west movements
475 along the fault ([Figure 3Figure 3e](#)).

476 Pre-Pennsylvanian dykes

477 In the hanging wall and on the eastern flank of the folded Kongsfjorden–Cowanodden fault
478 zone in Nordmannsfonna, high- to low-amplitude, gently east-dipping seismic reflections, which
479 possibly represent sedimentary strata (light orange unit in [Figure 3Figure 3e](#)), are crosscut but not
480 offset by moderately west-dipping, high-amplitude planar reflections (blue lines in [Figure 3Figure](#)
481 [3e](#)). In NNE–SSW-trending cross-sections, these high-amplitude, cross-cutting seismic reflections
482 appear sub-horizontal (blue lines in [Figure 3Figure 3f](#)). These crosscutting, west-dipping
483 reflections are mildly folded in places and either terminate upwards within the suggested, gently
484 east-dipping, sedimentary strata (light orange unit in [Figure 3Figure 3e](#)) or are truncated by the
485 base-Pennsylvanian unconformity (white line in [Figure 3Figure 3e](#)). Downwards within the
486 Kongsfjorden–Cowanodden fault zone (black lines in [Figure 3Figure 3e](#)), these inclined reflections
487 can be vaguely traced as a series of discontinuous, subtle features (see blue lines in [Figure 3Figure](#)
488 [3e](#)). In the footwall of the Kongsfjorden–Cowanodden fault zone, the inclined reflections become
489 more prominent again, still do not offset background reflections, and extend to depths of 3–3.5
490 seconds (TWT; blue lines in [Figure 3Figure 3e](#)). The high amplitude of these planar west-dipping
491 reflections, the absence of offset across them, and their discontinuous geometries across the
492 Agardhbukta Fault and the Kongsfjorden–Cowanodden fault zone suggest that they may represent
493 dykes (see Phillips et al., 2018). Because they appear truncated by the Base-Pennsylvanian

494 unconformity, we suggest such dykes were emplaced prior to development of this unconformity.
495 The Kongsfjorden–Cowanodden fault zone is folded into a broad, 15–20 kilometers wide anticline,
496 and offset > 0.5 second (TWT) by the Agardhbukta Fault, whereas the west-dipping dykes (blue
497 lines in [Figure 3Figure 3e](#)) and the gently east-dipping sedimentary strata they intrude (light orange
498 unit in [Figure 3Figure 3e](#)) are only mildly folded and show no offset across the Agardhbukta Fault
499 ([Figure 3Figure 3e](#)). These differences in deformation suggest that the latter were deformed during
500 a mild episode of late contraction but not by the same early episode of intense contraction that
501 resulted in macrofolding of the Kongsfjorden–Cowanodden fault zone.

502 Cretaceous dykes and sills

503 Near or at the surface, thin, kilometer-wide, lenticular packages of gently dipping,
504 moderate–high-amplitude seismic reflections (black units in [Figure 3Figure 3e–f](#)) correlate with
505 surface outcrops of Cretaceous sills of the Diabasodden Suite in eastern Spitsbergen (Senger et al.,
506 2013; Dallmann, 2015). In places, these sills are associated with areas showing high-frequency
507 disruptions of underlying sub-horizontal seismic reflections (dotted black lines in [Figure 3Figure](#)
508 [3f](#)) correlated with onshore occurrences of Pennsylvanian–Mesozoic sedimentary strata (Andresen
509 et al., 1992; Haremo and Andresen, 1992; Dallmann, 2015). We interpret these areas of high-
510 frequency disruption in otherwise relatively undisturbed and only mildly deformed Pennsylvanian–
511 Mesozoic sedimentary strata as zones with occurrences of Cretaceous feeder dykes. Alternatively,
512 disruption may be related to scattering and attenuation of seismic energy caused on the sills.

513

514 *Stappen High (northwestern Norwegian Barents Sea north of Bjørnøya)*

515 On the Stappen High between Bjørnøya and Spitsbergen ([Figure 1Figure 1c](#)), seismic
516 reflections at depth of 2–6 seconds (TWT) are dominated by moderate- to high-amplitude
517 reflections with limited (< five kilometers) lateral continuity showing asymmetric, dominantly
518 SSW-leaning curving geometries with a few hundreds of meters to a few kilometers width (yellow
519 lines within pink unit in [Figure 3Figure 3c](#)), i.e., analogous to those in folded Precambrian
520 basement rocks farther north ([Figure 3Figure 3a](#) and [Figure 4Figure 4a](#)). These reflections are
521 truncated by gently to moderately NNE- (and subsidiary SSW-) dipping disruption surfaces (black
522 lines within pink and purple units in [Figure 3Figure 3c](#)), some of which connect upwards with
523 shallow (0–2 seconds TWT), NNE-dipping, high-angle listric disruptions near Bjørnøya in the
524 south (red lines in [Figure 3Figure 3c](#)). Notably, major seismic reflections near the upwards

525 termination of deep, moderately–gently NNE-dipping disruption surfaces display characteristic
526 gently curving-upwards geometries (yellow lines within pink and purple units in [Figure 3Figure](#)
527 [3c](#)) and overlying seismic onlaps (white half arrows in [Figure 3Figure 3c](#)) similar to those observed
528 just south of major NNE-dipping thrust systems in Storfjorden and the northeastern Norwegian
529 Barents Sea ([Figure 3Figure 3a](#) and supplement S2).

530 We interpret deep (2–6 seconds TWT), curving, discontinuous seismic reflections ((yellow
531 lines within pink and purple units in [Figure 3Figure 3c](#)) as folded Precambrian–lower Paleozoic
532 basement rocks, and dominantly NNE-dipping disruption surfaces (black lines within pink and
533 purple units in [Figure 3Figure 3](#)) as brittle–ductile thrust possibly partly mylonitic, though with
534 less intense deformation than the major NNE-dipping thrust systems observed farther north in
535 Storfjorden and the northeastern Norwegian Barents Sea, like the Kongsfjorden–Cowanodden fault
536 zone. These brittle–ductile thrusts can be traced eastwards on seismic data on the Stappen High
537 and into the Sørkapp Basin ([Figure 1Figure 1c](#)).

538 Based on their geometries and on gentle folding of the seafloor reflection (yellow lines
539 within green unit in [Figure 3Figure 3c](#)), shallow, NNE-dipping, high-angle listric disruptions are
540 interpreted as mildly inverted normal faults overprinting deep NNE-dipping thrusts. Based on
541 previous fieldwork on Bjørnøya (Worsley et al., 2001), on seismic mapping in the area (Lasabuda
542 et al., 2018), and on well tie to Hopen and Edgeøya, relatively continuous (> five kilometers)
543 shallow (0–2 seconds TWT), gently curved–undulating seismic reflections overlying folded
544 Precambrian–lower Paleozoic basement rocks are interpreted as mildly folded upper Paleozoic–
545 Mesozoic (–Cenozoic?) sedimentary strata (orange and green units in [Figure 3Figure 3c](#)).

546

547 ***Potential field data and regional gravimetric and magnetic anomalies***

548 *NNE-dipping thrusts*

549 In the northern Barents Sea, Storfjorden and central–eastern Spitsbergen, the seismic
550 occurrences of the Kongsfjorden–Cowanodden, Bellsundbanken and Kinnhøgda–
551 Daudbjørnpynten fault zones coincide with gradual, step-like, southwards increases in gravimetry
552 and, in places, with high magnetic anomalies in cross-section ([Figure 3Figure 3a–b](#) and [d–f](#)).
553 Similar southwards gradual and step-like increases in the Bouguer and magnetic anomalies
554 correlate with major thrusts north of Bjørnøya ([Figure 3Figure 3c](#); see [Figure 1Figure 1b](#) for
555 location of Bjørnøya). These patterns suggest that the footwall of the thrust systems consists of

556 relatively denser rock units, possibly with higher metamorphic grade. Seismic interpretation
557 showing thickening of metamorphosed and folded Precambrian basement rock units (pink unit in
558 Figure 3Figure 3a and c–d) in the footwall of the thrusts further support this claim.

559 In map-view gravimetric and magnetic data, the three thrust systems in Storfjorden (black
560 lines in Figure 3Figure 3a) coincide with three high, WNW–ESE-trending, continuous, gently
561 undulating (and, in place, merging/splaying) gravimetric and discontinuous magnetic anomalies
562 (dashed yellow lines in Figure 5Figure 5a–c) that are separated from each other by areas showing
563 relatively low gravimetric and magnetic anomalies (e.g., see green to blue areas in Figure 5Figure
564 5a). Some of these anomalies extend from central Spitsbergen to Storfjorden and the northern
565 Barents Sea (below the Ora and Olga basins) as curving, E–W- and NW–SE-trending, 50–100
566 kilometers wide anomalies (dashed yellow lines in Figure 5Figure 5a–c). Analogously, thrust
567 systems north of Bjørnøya (Figure 3Figure 3c) and north of the Ora and Olga basins (supplement
568 S2b) correlate with comparable WNW–ESE-trending, curving magnetic and gravimetric anomalies
569 (dashed yellow lines in Figure 5Figure 5a–c). The WNW–ESE-trending anomalies appear clearer
570 by using a slope-direction shader for gravimetric data, which accentuates the contrast between each
571 trend of anomalies (green and red areas in Figure 5Figure 5b).

572 Most of the recognized, regional WNW–ESE-trending magnetic and gravimetric anomalies
573 (dashed yellow lines in Figure 5Figure 5a–c) can be traced into the Russian Barents Sea where they
574 are linear and are crosscut by major N–S- to NNW–SSE-trending anomalies (dashed black and
575 white lines in Figure 5Figure 5a–c). Subtle WNW–ESE-trending magnetic and gravimetric
576 anomalies further extend onshore northwestern Russia (e.g., Kanin Peninsula and southern Novaya
577 Zemlya) where they correlate with major Timanian thrusts and folds, some of which are suspected
578 to extend thousands of kilometers between northwestern Russia and the Varanger Peninsula in
579 northern Norway (e.g., Trollfjorden–Komagelva Fault Zone and Central Timan Fault and
580 associated Mikulkin Antiform; Siedlecka, 1975; Siedlecka and Roberts, 1995; Olovyanishnikov et
581 al., 2000; Lorenz et al., 2004; Kostyuchenko et al., 2006). In addition, two of the southernmost
582 WNW–ESE-trending gravimetric and magnetic anomalies coincide with the location of well
583 known, crustal-scale, SSW-verging Timanian thrust faults, the Trollfjorden–Komagelva Fault
584 Zone and the Central Timan Fault. Thus, based on their overall WNW–ESE trend, patterns of
585 alternating highs and lows both for gravimetric and magnetic anomalies (see Figure 5Figure 5a),
586 location at the boundary of oppositely dipping slopes (see slope-direction shader map in Figure

587 ~~5Figure 5b~~), and extensive field studies and seismic and well data in northwestern Russia (e.g.,
588 Kanin Peninsula and Timan Range; Siedlecka and Roberts, 1995; Olovyanishnikov et al., 2000;
589 ~~Lorenz et al., 2004~~; Kostyuchenko et al., 2006), ~~and~~ northern Norway (e.g., Varanger Peninsula;
590 Siedlecka, 1975), ~~and the southeastern Norwegian Barents Sea (Hassaan et al., 2021)~~, WNW–ESE-
591 trending anomalies are interpreted as a combination of basement-seated Timanian macrofolds and
592 top-SSW reverse faults (~~Figure 5Figure 5a–c~~).

593

594 *N–S-trending folds*

595 Large N–S-trending open folds (e.g., black and yellow lines in ~~Figure 3Figure 3b~~) coincide
596 with N–S- to NNE–SSW-trending, 20–100 kilometers wide, arcuate gravimetric and magnetic
597 anomalies (dashed white and black lines in ~~Figure 5Figure 5a–c~~), which are highly oblique to
598 WNW–ESE-trending gravimetric and magnetic anomalies and thrust systems (dashed yellow lines
599 in ~~Figure 5Figure 5a–c~~). Notably, major N–S- to NNE–SSW-trending synclines in ~~Figure 3Figure~~
600 ~~3b~~ (marked as red lines over a white line in ~~Figure 5Figure 5a~~ and c and as pink lines over a red
601 line in ~~Figure 5Figure 5b~~) coincides with similarly trending gravimetric and magnetic anomalies
602 (dashed black lines in ~~Figure 5Figure 5a~~ and c and dashed white lines in ~~Figure 5Figure 5b~~). On
603 the slope-direction shader map of gravimetric data, these N–S- to NNE–SSW-trending anomalies
604 are localized along the boundary between areas with eastwards- (ca. 90–100°; blue areas in ~~Figure~~
605 ~~5Figure 5b~~) and westwards-facing slopes (ca. 270–280°; white areas in ~~Figure 5Figure 5b~~).

606 Notably where the main thrusts are preserved, major N–S-trending synforms (see 50–60
607 kilometers wide U-shaped depression formed by the Kinnhøgda–Daudbjørnpynten fault zone, i.e.,
608 black lines, in ~~Figure 3Figure 3b~~) coincide with gravimetric and magnetic highs (white and black
609 dashed lines in ~~Figure 5Figure 5a–c~~), whereas major antiforms where major NNE-dipping thrusts
610 are partly eroded (e.g., c. 100 kilometers wide areas where the Kinnhøgda–Daudbjørnpynten fault
611 zone is absent in ~~Figure 3Figure 3b~~) coincide with gravimetric and magnetic lows (the lows are
612 parallel to white and black dashed lines symbolizing magnetic and gravimetric highs in ~~Figure~~
613 ~~5Figure 5a–c~~). The correlation of the interpreted NNE-dipping thrust systems with gravimetric
614 highs suggests that the thrusts consist of relatively denser rocks. This supports the inferred
615 mylonitic (*i.e., higher metamorphic grade*) component of the thrusts because mylonites are
616 relatively denser due to the formation of high-density minerals with increasing deformation (e.g.,
617 Arbaret and Burg, 2003; Colomby et al., 2015).

618 In the northwestern part of the Barents Sea (i.e., area covered by seismic data presented in
619 [Figure 3](#)Figure-3), N-S- to NNE-SSW-trending gravimetric and magnetic anomalies (white and
620 black dashed lines in [Figure 5](#)Figure-5a-c) are typically 20-50 kilometers wide and correlate with
621 similarly trending Caledonian folds and thrusts onshore Nordaustlandet (e.g., Rijpdalen Anticline;
622 Johansson et al., 2004; 2005; Dumais and Brønner, 2020) and northeastern Spitsbergen (e.g.,
623 Atomfjella Antiform; Gee et al., 1994; Witt-Nilsson et al., 1998), whose width is comparable to
624 that of the anomalies. In the south, N-S- to NNE-SSW-trending gravimetric and magnetic
625 anomalies merge together and swing into a NE-SW trend onshore-nearshore the Kola Peninsula
626 and northern Norway. These anomalies mimic the attitude of Caledonian thrusts and folds in the
627 southern Norwegian Barents Sea (Gernigon and Brønner, 2012; Gernigon et al., 2014) and onshore
628 northern Norway (Sturt et al., 1978; Townsend, 1987; Roberts and Williams, 2013). In the east, N-
629 S- to NNE-SSW-trending anomalies broaden to up to 150 kilometers in the Russian Barents Sea
630 ([Figure 5](#)Figure-5a-c).

631 In places, the intersections of high, WNW-ESE- and N-S- to NNE-SSW-trending
632 gravimetric and magnetic anomalies generate relatively higher, oval-shaped anomalies (e.g., dotted
633 white lines in [Figure 5](#)Figure-5a and c). Notable examples are found in the Ora and Olga basins
634 and east and south of these basins (see dotted white lines in [Figure 5](#)Figure-5a and c).

635

636 **Discussion**

637 In the discussion, we consider the lateral extent of the interpreted NNE-dipping thrust
638 systems, their possible timing of formation, and potential episodes of reactivation and overprinting.
639 Then we briefly discuss the implications of these thrust systems for plate tectonics reconstructions
640 in the Arctic.

641

642 ***Extent of NNE-dipping thrust systems***

643 Four major NNE-dipping systems of mylonitic thrusts and shear zones (Steiløya-Krylen,
644 Kongsfjorden-Cowanodden, Bellsundbanken, Kinnhøgda-Daudbjørnpynten fault zones) were
645 identified at depths > 1-2 seconds (TWT) in central-eastern Spitsbergen, Storfjorden and the
646 northeastern Barents Sea, and several systems with less developed ductile fabrics between
647 Spitsbergen and Bjørnøya on the Stappen High ([Figure 3](#)Figure-3a-f).

648 The Kongsfjorden–Cowanodden fault zone is relatively easy to trace and correlate in
649 Sassenfjorden, Sassendalen, Nordmannsfonna, Storfjorden and the northeastern Barents Sea (east
650 of Edgeøya) because (i) the seismic data in the these areas have a high resolution and good
651 coverage, (ii) internal seismic reflections are characterized by high amplitudes (e.g., brittle–ductile
652 thrusts and mylonitic shear zones), (iii) kinematic indicators within the thrust system consistently
653 show dominantly top-SSW sense of shear with SSW-verging fold structures ([Figure 3](#)[Figure 3a](#)
654 and d–f, and supplement S2), (iv) the geometry and kinematics indicators along shallow brittle
655 overprints are regionally consistent (listric, down-NNE, brittle normal faults; [Figure 3](#)[Figure 3a](#)
656 and d–f), and (v) this thrust consistently coincides with increase in gravimetric and magnetic
657 anomaly in cross-section ([Figure 3](#)[Figure 3a](#) and d) and with analogously trending gravimetric and
658 magnetic anomalies in central–eastern Spitsbergen and the northern Barents Sea ([Figure 5](#)[Figure](#)
659 [5a–b](#)). This thrust system was previously identified below the Ora Basin by Klitzke et al. (2019),
660 though interpreted as potential Timanian grain instead of a discrete structure. The proposed
661 correlation based on seismic, and cross-section and map-view gravimetric and magnetic data
662 suggests a lateral extent of c. 550–600 kilometers along strike for the Kongsfjorden–Cowanodden
663 fault zone. However, the regional magnetic and gravimetric anomalies associated with this thrust
664 in the Norwegian Barents Sea and Svalbard extend potentially farther east as a series of WNW–
665 ESE-trending anomalies to the mainland of Russia ([Figure 5](#)[Figure 5a–c](#)). Notably, these anomalies
666 correlate with the southern edge of Novaya Zemlya ([Figure 5](#)[Figure 5a–c](#)) and, more specifically,
667 with WNW–ESE-striking fault segments of the Baidaratsky fault zone ([Figure 1](#)[Figure 1a](#); Lopatin
668 et al., 2001; Korago et al., 2004), a major thrust fault that bounds a major basement high in the
669 central Russian Barents Sea, the Ludlov Saddle (Johansen et al., 1992; Drachev et al., 2010). Thus,
670 it is possible that the Kongsfjorden–Cowanodden fault zone also extends farther east, possibly
671 merging with the Baidaratsky fault zone, i.e., with a minimum extent of 1700–1800 kilometers
672 ([Figure 5](#)[Figure 5a–c](#)). This is supported by a similar configuration of the Baidaratsky Fault Zone
673 and the Kongsfjorden–Cowanodden fault zone, including a basement-seated, low-angle thrust
674 geometry of both faults and inversion as a normal fault and deposition of several seconds (TWT)
675 thick sedimentary strata in the hanging wall of the faults in the late Paleozoic (Figure 3d and
676 Smelror et al., 2009 their profile C–D pp. 53).

677 The overall NNE-dipping and folded (into NNE-plunging folds) geometry of the
678 Kongsfjorden–Cowanodden fault zone ([Figure 3](#)[Figure 3e–f](#) and Klitzke et al., 2019, their figures

679 3–5) may explain the alternating NW–SE- and E–W-trending geometry of the gravimetric and
680 magnetic anomalies correlating with this thrust system ([Figure 5Figure 5a–b](#)). E–W- and NW–SE-
681 trending segments of these anomalies may represent respectively the western and eastern limbs of
682 open, gently NNE-plunging macro-anticlines in the northern Norwegian Barents Sea. The
683 relatively higher, oval-shaped gravimetric and magnetic anomalies at the intersection of WNW–
684 ESE- and N–S- to NNE–SSW-trending magnetic and gravimetric highs, which are interpreted as
685 the interaction of two sub-orthogonal fold trends further support this claim ([Figure 5Figure 5a](#) and
686 c).

687 Interpretation of seismic sections ([Figure 3Figure 3e–f](#) and supplement S2) and regional
688 magnetic and gravimetric data ([Figure 5Figure 5a–c](#)) in central–eastern Spitsbergen show that
689 NNE-dipping, top-SSW Kongsfjorden–Cowanodden and Bellsundbanken fault zones likely extend
690 westwards into central (and possibly northwestern) Spitsbergen (e.g., Sassendalen, Sassenfjorden,
691 Tempelfjorden, and Billefjorden; see [Figure 1Figure 1c](#) for locations). This is further supported by
692 recent field, bathymetric and seismic mapping in central Spitsbergen showing that (inverted)
693 Devonian–Carboniferous NNE-dipping brittle normal faults in Billefjorden and Sassenfjorden–
694 Tempelfjorden merge with kilometer-scale, NNE-dipping, Precambrian basement fabrics and shear
695 zones at depth (Koehl, 2020a; Koehl et al., 2021 in review). Other examples of WNW–ESE-
696 trending fabrics include faults within Precambrian basement and Carboniferous sedimentary rocks
697 in northeastern Spitsbergen (Witt-Nilsson et al., 1998; Koehl and Muñoz-Barrera, 2018), and
698 within Devonian sedimentary rocks in northern and northwestern Spitsbergen (Friend et al., 1997;
699 McCann, 2000; Dallmann and Piepjohn, 2020). These suggest a repeated and regional influence of
700 WNW–ESE-trending thrust systems and associated basement fabrics in Spitsbergen.

701 Analogously to the Kongsfjorden–Cowanodden fault zone, the Bellsundbanken and
702 Kinnhøgda–Daudbjørnpynten fault zones ([Figure 3Figure 3a](#)) geometries and kinematics on
703 seismic data, and their coinciding with parallel gravimetric and magnetic anomalies in map view
704 and with magnetic and gravimetric highs in cross-section suggest that they extend from Storfjorden
705 to the island of Hopen ([Figure 1Figure 1c](#), [Figure 3Figure 3a](#), [Figure 5Figure 5a–c](#), and supplement
706 S2). Notably, a 50–100 kilometers wide, NNE–SSW-trending gravimetric and associated magnetic
707 anomaly interpreted as Caledonian grain in Nordaustlandet (Rijpdalen Anticline; Dumais and
708 Brønner, 2020) bends across the trace of these two thrust systems ([Figure 5Figure 5a–c](#)). Farther
709 east, the Bellsundbanken and Kinnhøgda–Daudbjørnpynten fault zones parallel gravimetric and

710 magnetic, alternating E–W- and NW–SE-trending anomalies that follow the trends and map-view
711 shapes of the Ora and Olga basins in the northeastern Norwegian Barents Sea (Anell et al., 2016;
712 see [Figure 1](#)[Figure 1b–c](#) for location). This suggests that these two thrust systems extend into the
713 northeastern Norwegian Barents Sea and, potentially, into the Russian Barents Sea, and affected
714 the development of Paleozoic sedimentary basins. This is also the case of the Steiløya–Krylen fault
715 zone (supplement S2b), which coincides with mild, discontinuous, WNW–ESE-trending
716 gravimetric and magnetic anomalies that extend well into the Russian Barents Sea and, possibly,
717 across Novaya Zemlya ([Figure 5](#)[Figure 5a–c](#)).

718 In southwestern Spitsbergen, field mapping revealed the presence of a major, subvertical,
719 kilometer-thick, WNW–ESE-striking mylonitic shear zone metamorphosed under amphibolite
720 facies conditions, the Vimsodden–Kosibapasset Shear Zone (Majka et al., 2008, 2012; Mazur et
721 al., 2009; see [Figure 1](#)[Figure 1c](#) for location). This major sinistral shear zone aligns along a WNW–
722 ESE-trending axis with the Kinnhøgda–Daudbjørnpynten fault zone in the northwestern
723 Norwegian Barents Sea ([Figure 3](#)[Figure 3a](#)), and shows a folded geometry in map view that is
724 comparable to that of major NNE-dipping thrust systems in the northern Norwegian Barents Sea
725 ([Figure 3](#)[Figure 3a](#) and e–f, [Figure 5](#)[Figure 5a–c](#), and supplement S2; Klitzke et al., 2019). In
726 addition, the Vimsodden–Kosibapasset Shear Zone juxtaposes relatively old Proterozoic basement
727 rocks in the north against relatively young rocks in the south, thus suggesting a similar
728 configuration and kinematics as along the Kinnhøgda–Daudbjørnpynten fault zone in Storfjorden
729 and the northeastern Norwegian Barents Sea. Moreover, von Gosen and Piepjohn (2001) and Bergh
730 and Grogan (2003) reported that Devonian–Mississippian sedimentary successions and Cenozoic
731 fold structures (e.g., Hyrnefjellet Anticline) are offset sinistrally by a few kilometers in Hornsund.
732 Thus, we propose that the Vimsodden–Kosibapasset Shear Zone extends into Hornsund and
733 represents the westwards continuation of the Kinnhøgda–Daudbjørnpynten fault zone. This
734 suggests a minimum extent of 400–450 kilometers for this thrust system ([Figure 1](#)[Figure 1b–c](#) and
735 [Figure 5](#)[Figure 5a–c](#)).

736

737 ***Timing of formation of major NNE-dipping thrust systems and N–S-trending folds***

738 *NNE-dipping thrust systems*

739 The several-kilometer thickness and hundreds–thousands of kilometers along-strike extent
740 of NNE-dipping thrust systems in central–eastern Spitsbergen, Storfjorden, and the northwestern

741 and northeastern Norwegian Barents Sea suggest that they formed during a major contractional
742 tectonic event. The overall WNW–ESE trend and the consistent north-northeastwards dip and top-
743 SSW sense of shear along the newly evidenced deep thrust systems preclude formation during the
744 Grenvillian, Caledonian, and Ellesmerian orogenies, and the Eurekan tectonic event. These tectonic
745 events all involved dominantly E–W-oriented contraction and resulted in the formation of overall
746 N–S- to NNE–SSW-trending fabrics, structures and deformation belts in Svalbard (i.e., sub-
747 orthogonal to the newly identified thrust systems) such as the Atomfjella Antiform (Gee et al.,
748 1994; Witt-Nilsson et al., 1998), the Vestfonna and Rijpdalen anticlines (Johansson et al., 2004;
749 2005; Dumais and Brönnér, 2020), the Dickson Land and Germaniahelvøya fold-thrust zones
750 (McCann, 2000; Piepjohn, 2000; Dallmann and Piepjohn, 2020), and the West Spitsbergen Fold-
751 and-Thrust Belt and related early Cenozoic structures in eastern Spitsbergen (Andresen et al., 1992;
752 Haremo and Andresen, 1992; Dallmann et al., 1993), and NE–SW- to NNE–SSW-striking thrusts
753 and folds in northern Norway (Sturt et al., 1978; Townsend, 1987; Roberts and Williams, 2013)
754 and the southwestern Barents Sea (Gernigon et al., 2014).

755 A possible cause for the formation of the observed NNE-dipping thrust systems is the late
756 Neoproterozoic Timanian Orogeny, which is well known onshore northwestern Russia (e.g., Kanin
757 Peninsula, Timan Range and central Timan; Siedlecka and Roberts, 1995; Olovyanishnikov et al.,
758 2000; [Lorenz et al., 2004](#); Kostyuchenko et al., 2006) and northeastern Norway (Varanger
759 Peninsula; Siedlecka and Siedlecki, 1967; Siedlecka, 1975; Roberts and Olovyanishnikov, 2004),
760 and traces of which were recently found [in the southeastern Norwegian Barents Sea \(Hassaan et](#)
761 [al., 2020a, 2020b, 2021; Hassaan, 2021\)](#), in southwestern Spitsbergen (Majka et al., 2008, 2012,
762 2014) and northern Greenland (Rosa et al., 2016; Estrada et al., 2018). The overall transport
763 direction during this orogeny was directed towards the south-southwest and most thrust systems
764 show NNE-dipping geometries (Olovyanishnikov et al., 2000; [Lorenz et al., 2004](#); Kostyuchenko
765 et al., 2006), e.g., the Timanian thrust front on the Varanger Peninsula in northeastern Norway
766 (Trollfjorden–Komagelva Fault Zone; Siedlecka and Siedlecki, 1967; Siedlecka, 1975) [and its](#)
767 [eastwards continuation, the Central Timan Fault \(Lorenz et al., 2004; Kostyuchenko et al., 2006\)](#).
768 In addition, the size of Timanian thrust systems [and related thrust anticlines](#) in the Timan Range
769 [and Kanin Peninsula](#) (e.g., Central Timan Fault [and Mikulkin Antiform](#)) ~~is-are~~ comparable (≥ 3 –4
770 seconds TWT [thick thrusts and 5–15 kilometers wide thrust-related major anticlines](#); [Lorenz et al.](#),

771 2004 their figures 3 and 5; Kostyuchenko et al., 2006 their figure 17) to that of thrust and fold
772 systems in the northern Norwegian Barents Sea and Svalbard (Figure 3Figure 3a and c–d).

773 Thus, based on their overall WNW–ESE strike (Figure 1Figure 1b–c), their vergence to the
774 south-southwest (Figure 3Figure 3a, c–d and f), their coincidence with gravimetric and magnetic
775 highs (Figure 5Figure 5a–c), their upward truncation by a major unconformity consistently
776 throughout the study area (see top-Precambrian unconformity in Figure 3Figure 3a–d), and the
777 correlation of these NNE-dipping thrusts and associated major anticlines (via gravimetric and
778 magnetic anomalies) to similarly striking and verging structures of comparable size (i.e., several
779 seconds TWT thick, 5–15 kilometers wide anticlines) onshore–nearshore northwestern Russia and
780 northern Norway (Siedlecka, 1975; Siedlecka and Roberts, 1995; Olovyanishnikov et al., 2000;
781 Roberts and Siedlecka, 2002; Lorenz et al., 2004; Gee and Pease, 2004; Kostyuchenko et al., 2006),
782 NNE-dipping thrusts in the northern Norwegian Barents Sea, Storfjorden, and central–eastern
783 Spitsbergen are interpreted as the western continuation of Timanian thrust and fold systems.

784 Timanian grain was recently identified in the northeastern Norwegian Barents Sea through
785 interpretation of new seismic, magnetic and gravimetric datasets shown in Figure 5Figure 5a–c
786 (Klitzke et al., 2019). The alignment, coincident location, and matching geometries (e.g., curving
787 E–W to NW–SE strike/trend and kilometer-wide NNE–SSW-trending anticline) between Timanian
788 grain and structures mapped by Klitzke et al. (2019) and the major, NNE-dipping, top-SSW thrust
789 systems described in central–eastern Spitsbergen, Storfjorden and the Norwegian Barents Sea
790 (Figure 3Figure 3a–f and supplement S2) further support a Timanian origin for the latter. Further
791 evidence of relic Timanian structural grain as far as the Loppa High and Bjørnøya Basin are
792 documented by previous magnetic studies and modelling (Marello et al., 2010). Moreover, seismic
793 mapping suggests that Timanian thrust systems extend well into central Spitsbergen (Figure
794 3Figure 3e–f and supplement S2c–d; Koehl, 2020a; Koehl et al., 2021 in review), and regional
795 gravimetric and magnetic anomaly maps suggest that Timanian thrust systems might extend farther
796 west to (north-) western Spitsbergen (Figure 5Figure 5a–c).

797 Probable reasons as to why these major (hundreds–thousands of kilometers long) thrust
798 systems were not identified before during fieldwork in Svalbard are their burial to high depth (>
799 1–2 seconds TWT in the study area, i.e., several kilometers below the surface; Figure 3Figure 3a–
800 f), and their strong overprinting by younger tectonic events like the Caledonian Orogeny in areas
801 where they are exposed (e.g., Vimsodden–Kosibapasset Shear Zone in southwestern Spitsbergen;

802 Faehnrich et al., 2020). Possible areas of interest for future studies include the western and
803 northwestern parts of Spitsbergen where Caledonian and Eureka E–W contraction contributed to
804 uplift and exhume deep basement rocks, and where Timanian rocks potentially crop out (e.g.,
805 Peucat et al., 1989).

806

807 *N–S-trending folds*

808 N–S-trending upright folds involve the NNE-dipping thrust systems ([Figure 3](#)[Figure-3b](#) and
809 e) and correlate (via gravimetric and magnetic anomalies) with major Caledonian folds in
810 northeastern Spitsbergen and Nordaustlandet, like the Atomfjella Antiform (Gee et al., 1994; Witt-
811 Nilsson et al., 1998) and Rijpdalen Anticline (Johansson et al., 2004; 2005; Dumais and Brönnér,
812 2020), with Caledonian grain in the southern Norwegian Barents Sea (Gernigon and Brönnér, 2012;
813 Gernigon et al., 2014), and with major NE–SW-trending Caledonian folds onshore northern
814 Norway (Sturt et al., 1978; Townsend, 1987; Roberts and Williams, 2013). In addition, the width
815 of the NE–SW- to N–S-trending gravimetric and magnetic anomalies associated with these folds
816 increases up to 150 kilometers eastwards, i.e., away from the Caledonian collision zone ([Figure](#)
817 [5](#)[Figure-5a-c](#); Corfu et al., 2014; Gasser, 2014). Thus, N–S-trending folds in the northern
818 Norwegian Barents Sea are interpreted as Caledonian regional folds in Precambrian–lower
819 Paleozoic rocks. The relatively broader geometry of Caledonian folds away from the Caledonian
820 collision zone (e.g., in the Russian Barents Sea) is inferred to be related to gentler fold geometries
821 due to decreasing deformation intensity in this direction. This is further supported by relatively low
822 grade Caledonian metamorphism in Franz Josef Land (Knudsen et al., 2019; see [Figure 1](#)[Figure](#)
823 [4a-b](#) for location). By contrast, the presence of tighter Caledonian folds near the collision zone in
824 the northern Norwegian Barents Sea (e.g., [Figure 3](#)[Figure-3b](#) and e, and Atomfjella Antiform and
825 Rijpdalen Anticline onshore; Gee et al., 1994; Witt-Nilsson et al., 1998; Johansson et al., 2004,
826 2005; Dumais and Brönnér, 2020) is associated with much narrower (20–50 kilometers wide)
827 gravimetric and magnetic anomalies ([Figure 5](#)[Figure-5a-c](#)). Note that the Atomfjella Antiform and
828 Rijpdalen Anticline can be directly correlated with 20–50 kilometers wide, N–S-trending high
829 gravimetric and magnetic anomalies ([Figure 5](#)[Figure-5a-c](#)). Noteworthy, some of the NNE–SSW-
830 trending folds and anomalies in the northernmost Norwegian Barents Sea may reflect a
831 combination of Caledonian and superimposed early Cenozoic Eureka folding (e.g., Kairanov et
832 al., 2018).

833 The interference of WNW–ESE- and N–S- to NNE–SSW-trending gravimetric highs,
834 which are correlated to Timanian and Caledonian folds respectively, produces oval-shaped
835 gravimetric and magnetic highs ([Figure 5](#)~~Figure 5~~a). These relatively higher, oval-shaped
836 gravimetric anomalies are interpreted to correspond to dome-shaped folds resulting from the
837 interaction of Timanian and Caledonian folds involving refolding of WNW–ESE-trending
838 Timanian folds during E–W Caledonian contraction. Field studies on the Varanger Peninsula in
839 northern Norway and seismic studies of Timanian thrusts off northern Norway where the
840 interaction of Timanian and Caledonian folds produced dome-shaped fold structures (Ramsay,
841 1962), e.g., like the Ragnarokk Anticline (Siedlecka and Siedlecki, 1971; Koehl, in prep.) also
842 support this interpretation. Furthermore, Barrère et al. (2011) suggested that basins and faults in
843 the southern Norwegian Barents Sea are controlled by the interaction of Caledonian and Timanian
844 structural grain, and Marelllo et al. (2010) argued that elbow-shaped magnetic anomalies reflect the
845 interaction of Caledonian and Timanian structural grains in the Barents Sea, potentially as far west
846 as the Loppa High and the Bjørnøya Basin.

847

848 ***Phanerozoic reactivation and overprinting of Timanian thrust systems***

849 *Caledonian reactivation and overprint*

850 The geometry of the Kongsfjorden–Cowanodden and Kinnhøgda–Daudbjørnpynten fault
851 zones in Nordmannsfonna ([Figure 3](#)~~Figure 3~~e) and in the northeastern Norwegian Barents Sea
852 ([Figure 3](#)~~Figure 3~~b; Klitzke et al., 2019), where they are folded into broad NNE-plunging upright
853 anticlines and synclines suggests that these thrust systems were deformed after they accommodated
854 top-SSW Timanian thrusting ([Figure 6](#)~~Figure 6~~a and [Figure 7](#)~~Figure 7~~a). In addition, subsidiary
855 top-west kinematics (west-verging folds and top-west minor thrusts) suggest that ~~these~~ Timanian
856 thrust systems were partly reactivated–overprinted during an episode of intense E–W contraction
857 ([Figure 6](#)~~Figure 6~~b and [Figure 7](#)~~Figure 7~~b). However, west-dipping dykes crosscutting and gently
858 east-dipping sedimentary strata overlying the eastern part of the folded Kongsfjorden–
859 Cowanodden fault zone are only mildly folded, and upper Paleozoic sedimentary strata lie flat over
860 folded and partly eroded Precambrian–lower Paleozoic rocks and the Kinnhøgda–
861 Daudbjørnpynten fault zone, thus suggesting that these sedimentary strata and dykes were not
862 involved in this episode of E–W contraction ([Figure 3](#)~~Figure 3~~e).

863 A notable episode of E–W contraction in Svalbard is the Caledonian Orogeny in the early–
864 mid Paleozoic, which resulted in the formation of west-verging thrusts and N–S-trending folds of
865 comparable size (c. 15–25 kilometers wide) to those affecting the Kongsfjorden–Cowanodden and
866 Kinnhøgda–Daudbjørnpynten fault zones in Nordmannsfonna and the northern Norwegian Barents
867 Sea (Figure 3b and e; Klitzke et al., 2019, their figures 3–5), such as the Atomfjella
868 Antiform in northeastern Spitsbergen (Gee et al., 1994; Witt-Nilsson et al., 1998; Lyberis and
869 Manby, 1999) and the Rijpdalen Anticline in Nordaustlandet (Figure 1b). Since the NNE-
870 plunging anticline in Nordmannsfonna does not affect overlying Pennsylvanian–Mesozoic
871 sedimentary strata (Figure 3e), we propose that they formed during Caledonian contraction
872 (Figure 7b). This is supported by the involvement of the top-Precambrian unconformity
873 and underlying NNE-dipping thrusts in N–S- to NNE-SSW-trending folds, and by the truncation
874 of these folds by the top-Silurian unconformity, which is overlapped by mildly deformed to flat-lying
875 upper Paleozoic strata (Figure 3b and Figure 4f). Furthermore, structures with
876 geometries comparable to NNE-plunging folds in the northern Barents Sea and Svalbard were
877 observed in northern Norway. An example is the Ragnarokk Anticline, a dome-shaped fold
878 structure along the Timanian front thrust on the Varanger Peninsula, which results from the re-
879 folding of Timanian thrusts and folds into a NE–SW-trending Caledonian trend (Siedlecka and
880 Siedlecki, 1971).

881 Further support of a Caledonian origin for upright NNE-plunging folds in eastern
882 Spitsbergen, Storfjorden and the northern Norwegian Barents Sea is that these folds are relatively
883 tight in the west, in Nordmannsfonna and the northwestern Barents Sea (Figure 3b and e),
884 whereas they show gradually gentler and more open geometries in the east, i.e., away from the
885 Caledonian collision zone (Figure 3b). This is also shown by the gradual eastwards
886 broadening of regional gravimetric and magnetic anomalies correlated with Caledonian folds
887 suggesting gentler fold geometries related to decreasing (Caledonian) deformation intensity in this
888 direction (Figure 5a–c). This contrasts with the homogeneous intensity of deformation
889 along NNE-dipping thrusts on seismic data and with the homogeneous width of related
890 gravimetric–magnetic anomalies from west to east in Svalbard and the Barents Sea (Figure 3a–f
891 and Figure 5a–c and supplement S2). Caledonian folding of Timanian thrusts also
892 explains the weaker magnetic and gravimetric signal of Timanian faults at the location of major
893 Caledonian synclines where Timanian faults were transported downwards and, therefore, may not

894 show well on potential field data (e.g., major two, NE–SW- to N–S-trending, negative gravimetric
895 anomalies in the Russian Barents Sea just west of Novaya Zemlya; Figure 5a).

896 In Nordmannsfonna, the Caledonian origin of the major 15–20 kilometers wide anticline,
897 and the truncation of overlying, gently east-dipping, mildly folded sedimentary strata and
898 crosscutting west-dipping dykes by the base-Pennsylvanian unconformity suggest that these
899 sedimentary strata and dykes are Devonian (–Mississippian?) in age (Figure 6Figure 6c–d). This is
900 supported by the presence of thick Devonian–Mississippian collapse deposits in adjacent areas of
901 central–northern Spitsbergen (Cutbill et al., 1976; Murascov and Mokin, 1979; Aakvik, 1981;
902 Gjelberg, 1983; Manby and Lyberis, 1992; Friend et al., 1997), and by Middle Devonian to
903 Mississippian ages (395–327 Ma) for dykes in central–northern Spitsbergen (Evdokimov et al.,
904 2006), northern Norway (Lippard and Prestvik, 1997; Guise and Roberts, 2002), and northwestern
905 Russia (Roberts and Onstott, 1995).

906 The occurrence of a > 0.5 second (TWT) reverse offset of the folded Kongsfjorden–
907 Cowanodden fault zone and the lack of offset of the Devonian (–Mississippian?) dykes across the
908 Agardhbukta Fault indicate that the latter fault formed as a top-west thrust during the Caledonian
909 Orogeny. At depth, the Agardhbukta Fault merges with the eastern flank of the folded
910 Kongsfjorden–Cowanodden fault zone. This, together with the presence of minor, high-angle, top-
911 west brittle thrusts within the Kongsfjorden–Cowanodden fault zone (Figure 3Figure 3e), indicates
912 that the Agardhbukta Fault reactivated and/or overprinted the eastern portion of the Kongsfjorden–
913 Cowanodden fault zone in Nordmannsfonna during Caledonian contraction (Figure 6Figure 6b and
914 Figure 7Figure 7b). Depth conversion using seismic velocities from Gernigon et al. (2018) suggest
915 that the Agardhbukta Fault offset the Kongsfjorden–Cowanodden fault zone by ca. 2.4–2.5
916 kilometers top-west during Caledonian contraction (Figure 3Figure 3e and supplement S3g). These
917 kinematics are consistent with field observation in eastern Spitsbergen by Piepjohn et al. (2019,
918 their figure 17b). However, Piepjohn et al. (2019) also suggested a significant component of
919 Mesozoic–Cenozoic, down-east normal movement, which was not identified on seismic data in
920 Nordmannsfonna. This suggests either along strike variation in the movement history of the
921 Agardhbukta Fault, either that the fault mapped on seismic data in Nordmannsfonna does not
922 correspond to the Agardhbukta Fault of Piepjohn et al. (2019).

923 Considering the presence of crustal-scale, NNE-dipping, hundreds (to thousands?) of
924 kilometers long (Timanian) thrust systems extending from the Barents Sea (and possibly from

925 onshore Russia) to central–eastern and southern Spitsbergen and the northwestern Norwegian
926 Barents Sea (Figure 5a–c) prior to the onset of E–W-oriented Caledonian contraction, it is
927 probable that such large structures would have (at least partially) been reactivated and/or
928 overprinted during subsequent tectonic events if suitably oriented. Under E–W contraction, WNW–
929 ESE-striking, dominantly NNE-dipping Timanian faults would be oriented at c. 30° to the direction
930 of principal stress and, therefore, be suitable (according to Anderson’s stress model) to
931 reactivate/be overprinted with sinistral strike-slip movements. Such kinematics were recorded
932 along the Vimsodden–Kosibapasset Shear Zone in Wedel Jarlsberg Land (Mazur et al., 2009) and
933 within Hornsund (von Gosen and Piepjohn, 2001).

934 However, recent ^{40}Ar – ^{39}Ar geochronological determinations on muscovite within this
935 structure suggest that this structure formed during the Caledonian Orogeny (Faehnrich et al. 2020).
936 Nonetheless, the same authors also obtained Timanian ages (600–540 Ma) for (initial) movements
937 along minor shear zones nearby and parallel to the Vimsodden–Kosibapasset Shear Zone. Since
938 this large shear zone must have represented a major preexisting zone of weakness when Caledonian
939 contraction initiated, it is highly probable that it was preferentially chosen to reactivate instead of
940 minor shear zones. Thus, the Caledonian ages obtained along the Vimsodden–Kosibapasset Shear
941 Zone most likely reflect complete resetting of the geochronometer along the shear zone due to large
942 amounts of Caledonian reactivation–overprinting, while minor nearby shear zones preserved traces
943 of initial Timanian deformation. This is also supported by observations in northern Norway
944 suggesting that Timanian thrusts (e.g., Trollfjorden–Komagelva Fault Zone) were reactivated as
945 major strike-slip faults during the Caledonian Orogeny (Roberts, 1972; Herrevold et al., 2009; Rice
946 2014). This interpretation reconciles the strong differences in dipping angle and depth between the
947 Kinnhøgda–Daudbjørnpynten fault zone and the Vimsodden–Kosibapasset Shear Zone. The
948 former was located away from the Caledonian collision zone and essentially retained its initial,
949 moderately NNE-dipping Timanian geometry and was deeply buried during the Phanerozoic,
950 whereas the latter was intensely deformed, pushed into a sub-vertical position, and uplifted an
951 exhumed to the surface because it was located near or within the Caledonian collision zone.

952 This further explains why Timanian faults were not reactivated exclusively as strike-slip
953 faults despite being oriented sub-orthogonal (c. 70°) to E–W Caledonian contraction. Portions of
954 Timanian faults near the Caledonian collision zone were locally deformed into subvertical
955 geometries suitable to accommodate lateral movement, whereas their counterparts retaining their

956 moderate–low-angle dip away from the paleo-plate boundary were more prone to accommodate
957 vertical movements. Moreover, lateral transport of rocks from the Caledonian collision front
958 towards the inner portions of the Barents Sea in the east was hampered by rock units constituting
959 the crust of the Barents Sea, northern Norway, northwestern Russia and other adjacent areas.
960 Hence, Caledonian E–W contraction produced more easily N–S-trending folds (e.g., Figure 3b and
961 e and Figure 4f), which extended almost all the way to Novaya Zemlya (Figure 5), whereas partial
962 strike-slip reactivation was restricted to areas proximal to the Caledonian collision front (e.g.,
963 western Spitsbergen; Majka et al., 2008; Mazur et al., 2009; Faehnrich et al., 2020; Ziemniak et
964 al., 2020).

965

966 *Devonian–Carboniferous normal overprint–reactivation*

967 In Nordmannsfonna, the wedge shape of Devonian (–Mississippian?) sedimentary strata in
968 the hanging wall of the Kongsfjorden–Cowanodden fault zone suggest that the eastern portion of
969 this thrust was reactivated as a gently–moderately dipping extensional detachment (Figure 6Figure
970 6c) and, thus, that Devonian (–Mississippian?) strata in this area represent analogs to collapse
971 deposits in northern Spitsbergen. The intrusion of west-dipping Devonian (–Mississippian?) dykes
972 orthogonal to the eastern portion of the thrust system, i.e., orthogonal to extensional movements
973 along the inverted east-dipping portion of the thrust (Figure 3Figure 3e and Figure 6Figure 6d) also
974 supports this interpretation. Similar relationships were inferred in northwestern Spitsbergen, where
975 Devonian collapse sediments were deposited along a N–S-trending Precambrian basement ridge
976 bounded by a gently dipping, extensional mylonitic detachment (Braathen et al., 2018).

977 In Sassenfjorden, Storfjorden and the northeastern Norwegian Barents Sea, listric brittle
978 normal faults showing down-NNE offsets and syn-tectonic thickening within Devonian–
979 Carboniferous (–Permian?) sedimentary strata merge at depth with the uppermost part of NNE-
980 dipping Timanian thrust systems like the Kongsfjorden–Cowanodden fault zone (Figure 3Figure
981 3a and d and supplement S2c). This indicates that Timanian thrust systems were used as preexisting
982 zones of weakness during late–post-orogenic collapse of the Caledonides in the Devonian–
983 Carboniferous (Figure 6Figure 6c–e and Figure 7Figure 7c).

984 The presence of the Kongsfjorden–Cowanodden fault zone in Storfjorden and below
985 Edgeøya also explains the strong differences between the Paleozoic sedimentary successions
986 penetrated by the Plurdalen-1 and Raddendalen-1 exploration wells (Bro and Shvarts, 1983;

987 Harland and Kelly, 1997). Notably, the Plurdalen-1 well penetrated (at least) ca. 1600 meters thick
988 Devonian–Mississippian sedimentary rocks in the direct hanging wall of the Kongsfjorden–
989 Cowanodden fault zone and related listric brittle overprints ([Figure 3](#)~~Figure 3~~a), whereas the
990 interpretation of Bro and Shvarts (1983) suggests that the Raddedalen-1 well encountered thin (90–
991 290 meters thick) Mississippian strata overlying (> 2 kilometers) thick lower Paleozoic
992 sedimentary rocks ca. 30 kilometers farther northeast, i.e., away from the Kongsfjorden–
993 Cowanodden fault zone and related overprints. The presence of thick Devonian sedimentary strata
994 in the direct hanging wall of listric overprints of the Kongsfjorden–Cowanodden fault zone further
995 supports late–post-Caledonian extensional reactivation–overprinting of NNE-dipping Timanian
996 thrusts.

997 In central Spitsbergen, recently identified Early Devonian–Mississippian normal faults
998 formed along and overprinted–reactivated major NNE-dipping ductile (mylonitic) shear zones and
999 fabrics in Billefjorden (Koehl et al., 2021 in review) and Sassenfjorden–Tempelfjorden (Koehl,
1000 2020a). These show sizes, geometries and kinematics comparable to those of the Kongsfjorden–
1001 Cowanodden fault zone, and are, therefore, interpreted as the western continuation of this thrust
1002 system. The Devonian–Carboniferous extensional reactivation–overprinting of the Kongsfjorden–
1003 Cowanodden fault zone in central Spitsbergen explains the southward provenance of northwards
1004 prograding sedimentary rocks of the uppermost Silurian–Lower Devonian Siktefjellet and Red Bay
1005 groups and Wood Bay Formation and the enigmatic WNW–ESE trend of the southern boundary of
1006 the Devonian Graben in central–northern Spitsbergen (Gee and Moody-Stuart, 1966; Friend et al.,
1007 1966; Friend and Moody-Stuart, 1972; Murascov and Mokin, 1979; Friend et al., 1997; McCann,
1008 2000; Dallmann and Piepjohn, 2020; Koehl et al., 2021 in review).

1009

1010 *Mild Triassic overprint*

1011 The Kongsfjorden–Cowanodden fault zone and associated overprints align with WNW–
1012 ESE- to NW–SE-striking normal faults onshore southern and southwestern Edgeøya in
1013 Kvalpynten, Negerpynten, and Øhmanfjellet (Osmundsen et al., 2014; Ogata et al., 2018). These
1014 faults display both listric and steep planar geometries in cross-section and bound thickened syn-
1015 sedimentary growth strata in lowermost Upper Triassic sedimentary rocks of the Tschermakfjellet
1016 and De Geerdalen formations (Ogata et al., 2018; Smyrak-Sikora et al., 2020). The Norwegian
1017 Barents Sea and Svalbard are believed to have remained tectonically quiet throughout the Triassic

1018 apart from minor deep-rooted normal faulting in the northwestern Norwegian Barents Sea (Anell
1019 et al., 2013) and Uralides-related contraction in the (south-) east (Müller et al., 2019). Hence, we
1020 propose that the progradation and accumulation of thick sedimentary deposits of the Triassic deltaic
1021 systems above the southeastward continuation of the Kongsfjorden–Cowanodden fault zone may
1022 have triggered minor tectonic adjustments resulting in the development of a system of small half-
1023 grabens over the thrust system. Alternatively or complementary, the deposition of thick Triassic
1024 deltaic systems may have locally accelerated compaction of sedimentary strata underlying the
1025 Tschermakjellet Formation in south- and southwest-Edgeøya, e.g., of the potential pre-Triassic
1026 syn-tectonic growth strata along the Kongsfjorden–Cowanodden fault zone, and, thus, facilitated
1027 the development of minor half-grabens within the Triassic succession along this thrust system.

1028

1029 *Eurekan reactivation–overprint*

1030 In eastern Spitsbergen, the Agardhbukta Fault segment of the Lomfjorden Fault Zone
1031 truncates the Kongsfjorden–Cowanodden fault zone with a major, > 0.5 second (TWT) top-west
1032 reverse offset (Figure 3Figure–3e). The Agardhbukta fault also mildly folds Pennsylvanian–
1033 Mesozoic sedimentary rocks and Cretaceous sills into a gentle upright (fault-propagation) fold with
1034 no major offset (Figure 6Figure–6f–g), which is supported by onshore field observations in eastern
1035 and northeastern Spitsbergen (Piepjohn et al., 2019). Mild folding of Mesozoic sedimentary rocks
1036 and of Cretaceous intrusions indicates that the Agardhbukta Fault was most likely mildly
1037 reactivated as a top-west thrust during the early Cenozoic Eurekan tectonic event (Figure 6Figure
1038 6g and Figure 7Figure–7d).

1039 Seismic data show that high-angle listric Devonian–Carboniferous normal faults were
1040 mildly reactivated as reverse faults that propagated upwards and gently folded adjacent upper
1041 Paleozoic–Mesozoic (–Cenozoic?) sedimentary strata in the northwestern Norwegian Barents Sea,
1042 Storfjorden and central–eastern Spitsbergen (Figure 3Figure–3a–c and supplement S2), but not in
1043 the northeastern Norwegian Barents Sea (Figure 3Figure–3d). Since normal faults were not inverted
1044 in the east, it is probable that inversion of these faults in central–eastern Spitsbergen, Storfjorden
1045 and the northwestern Norwegian Barents Sea first occurred during the Eurekan tectonic event in
1046 the early Cenozoic, when Greenland collided with western Spitsbergen (Figure 7Figure–7d). This
1047 is also supported by the gently folded character of Devonian–Mesozoic (–Cenozoic?) sedimentary
1048 successions in the west (Figure 3Figure–3a and c), whereas these successions are essentially flat-

1049 lying (i.e., undeformed) in the east ([Figure 3](#)[Figure 3b](#) and [d](#)). Nevertheless, folding of the seafloor
1050 reflection in Storfjorden and the northwestern Norwegian Barents Sea suggests ongoing
1051 contractional deformation along several of these faults in the northwestern Norwegian Barents Sea
1052 and Storfjorden ([Figure 3](#)[Figure 3a–c](#)).

1053 Major, top-SSW mylonitic shear zones in Sassenfjorden–Tempelfjorden and Billefjorden
1054 display early Cenozoic overprints including top-SSW duplexes in uppermost Devonian–
1055 Mississippian coals of the Billefjorden Group acting as a partial décollement along a major
1056 basement-seated listric brittle fault (Koehl, 2020a; supplement S2) and NNE-dipping brittle faults
1057 offsetting the east-dipping Billefjorden Fault Zone by hundreds of meters to several kilometers left-
1058 laterally (Koehl et al., 2021 in review). Thus, the correlation of the Kongsfjorden–Cowanodden
1059 fault zone with these top-SSW mylonitic shear zones in Sassenfjorden–Tempelfjorden and
1060 Billefjorden (see [Figure 1](#)[Figure 1c](#) for location) supports reactivation–overprinting of major NNE-
1061 dipping Timanian thrust systems as top-SSW, sinistral-reverse, oblique-slip thrusts in the early
1062 Cenozoic Eureka tectonic event. Such correlation explains the NW–SE trend and the location of
1063 the northeastern boundary of the Central Tertiary Basin, which terminates just southwest of
1064 Sassenfjorden and Sassendalen in central Spitsbergen ([Figure 1](#)[Figure 1b–c](#)). It also explains the
1065 dominance of NW–SE- to WNW–ESE-striking faults within Cenozoic deposits of the Central
1066 Tertiary Basin (Livshits, 1965a), and the northwestwards provenance (Petersen et al., 2016) and
1067 northwards thinning of sediments deposited in the basin (Livshits, 1965b), which were probably
1068 sourced from uplifted areas in the hanging wall of the reactivated–overprinted thrust.

1069 Noteworthy, Livshits (1965a) argued that the Central Tertiary Basin was bounded to the
1070 north by a major WNW–ESE-striking fault extending from Kongsfjorden to southern Billefjorden–
1071 Sassenjorden where the NNE-dipping Kongsfjorden–Cowanodden fault zone was mapped (present
1072 study; supplement S2). This indicates that the Kongsfjorden–Cowanodden fault zone might extend
1073 west of Billefjorden and Sassenfjorden, potentially until Kongsfjorden (see [Figure 1](#)[Figure 1c](#) for
1074 location). Should it be the case, the Kongsfjorden–Cowanodden fault zone would coincide with a
1075 major terrane boundary in Svalbard, which was speculated to correspond to one or more regional
1076 WNW–ESE- to N–S-striking faults in earlier works, e.g., Kongsvegen Fault and Lapsdalen Thrust
1077 (Harland and Horsfield, 1974), Kongsvegen Fault Zone and/or Central–West Fault Zone (Harland
1078 and Wright, 1979), and Kongsfjorden–Hansbreen Fault Zone (Harland et al., 1993). The presence
1079 of a major, (inherited Timanian) NNE-dipping, basement-seated fault zone in this area would

1080 explain the observed strong differences between Precambrian basement rocks in Svalbard's
1081 northwestern and southwestern terranes.

1082 In southern Spitsbergen, von Gosen and Piepjohn (2001) and Bergh and Grogan (2003)
1083 suggested the presence of a WNW–ESE-striking, sinistral-reverse strike-slip fault in Hornsund
1084 based on a one-kilometer left-lateral offset of Devonian–Carboniferous sedimentary successions
1085 and of the early Cenozoic Hyrnefjellet Anticline across the fjord. This fault is part of the
1086 Kinnhøgda–Daudbjørnpynten fault zone and was most likely reactivated–overprinted during
1087 Eurekan contraction–transpression in the early Cenozoic.

1088

1089 *Present day tectonism*

1090 Seismic data show that the seafloor reflection is folded and/or offset in a reverse fashion by
1091 high-angle brittle faults merging at depth with interpreted Timanian thrust systems in Storfjorden
1092 and just north of Bjørnøya in the northwestern Norwegian Barents ([Figure 3](#)[Figure 3a](#) and [c](#), and
1093 [Figure 4](#)[Figure 4h](#)). This indicates that some of the Timanian thrust systems are still active at
1094 present and are reactivated/overprinted by reverse faults ([Figure 7](#)[Figure 7e](#)). A potential
1095 explanation for ongoing reactivation–overprinting is transfer of extensional tectonic stress in the
1096 Fram Strait as ridge-push tectonism through Spitsbergen and Storfjorden.

1097

1098 *Implication for plate tectonics reconstructions of the Barents Sea and Svalbard in the late* 1099 *Neoproterozoic–Paleozoic*

1100 The presence of hundreds to thousands of kilometers long Timanian faults throughout the
1101 northern Norwegian Barents Sea and central and southwestern (and possibly northwestern?)
1102 Spitsbergen indicates that the northwestern, northeastern and southwestern basement terranes of
1103 the Svalbard Archipelago were most likely already accreted together and attached to the Barents
1104 Sea, northern Norway and northwestern Russia in the late Neoproterozoic (ca. 600 Ma). Svalbard's
1105 three terranes were previously thought to have been juxtaposed during the Caledonian and
1106 Ellesmerian orogenies through hundreds–thousands of kilometers of displacement along presumed
1107 thousands of kilometers long N–S-striking strike-slip faults like the Billefjorden Fault Zone
1108 (Harland, 1969; Harland et al. 1992, Labrousse et al., 2008; [Figure 2](#)[Figure 2](#)). The presence of
1109 laterally continuous (undisrupted), hundreds–thousands of kilometers long, Timanian thrust

1110 systems from southwestern and central Spitsbergen to the northern Norwegian and Russian Barents
1111 Sea clearly shows that this is not possible (Figure 8Figure-8).

1112 The continuous character of these thrust systems from potentially as far as onshore
1113 northwestern Russia through the Barents Sea and Svalbard precludes any major strike-slip
1114 displacement along N–S-striking faults such as the Billefjorden Fault Zone and Lomfjorden Fault
1115 Zone (as proposed by Harland et al., 1974, 1992; Labrousse et al., 2008; Figure 2Figure-2) and any
1116 hard-linked connection between these faults in Svalbard and analogous, NE–SW-striking faults in
1117 Scotland in the Phanerozoic (as proposed by Harland, 1969). Instead, the present work suggests
1118 that the crust constituting the Barents Sea and the northeastern and southwestern basement terranes
1119 of Svalbard should be included as part of Baltica in future Arctic plate tectonics reconstructions for
1120 the late Neoproterozoic–Paleozoic period (i.e., until ca. 600 Ma; Figure 8Figure-8). It also suggests
1121 that the Caledonian suture zone, previously inferred to lie east of Svalbard in the Barents Sea (e.g.,
1122 Gee and Teben’kov, 2004; Breivik et al., 2005; Barrère et al., 2011; Knudsen et al., 2019) may be
1123 located west of the presently described Timanian thrust systems, i.e., probably west of or in western
1124 Spitsbergen where Caledonian blueschist and eclogite metamorphism has been recorded in
1125 Precambrian basement rocks (Horsfield, 1972; Dallmeyer et al., 1990a; Ohta et al., 1995;
1126 Kosminska et al., 2014).

1127

1128 **Conclusions**

- 1129 1) Seismic data in the northern Norwegian Barents Sea and Svalbard reveal the existence of
1130 several systems of hundreds–thousands of kilometers long, several kilometers thick, top-
1131 SSW thrusts comprised of brittle–ductile thrusts, mylonitic shear zones and associated
1132 SSW-verging folds that appear to extend from onshore northwestern Russia to the northern
1133 Norwegian Barents Sea and to central and southwestern Spitsbergen. A notable structure is
1134 the Kongsfjorden–Cowanodden fault zone in Svalbard and the Norwegian Barents Sea,
1135 which likely merges with the Baidaratsky fault zone in the Russian Barents Sea and
1136 southern Novaya Zemlya. We interpret these thrust systems as being related to the
1137 Neoproterozoic Timanian Orogeny.
- 1138 2) In the east (away from the Caledonian collision zone), these Timanian thrusts systems were
1139 folded into NNE-plunging folds, offset, and reactivated as and/or overprinted by top-west,
1140 oblique-slip sinistral-reverse, brittle–ductile thrusts during subsequent Caledonian (e.g.,

1141 Agardhbukta Fault segment of the Lomfjorden Fault Zone) and, possibly, during Eurekan
1142 contraction, and are deeply buried. By contrast, in the west (near or within the Caledonian
1143 collision zone), Timanian thrusts were intensely deformed, pushed into sub-vertical
1144 positions, extensively overprinted, and exhumed to the surface.

1145 3) In eastern Spitsbergen, a major NNE-dipping Timanian thrust system, the Kongsfjorden–
1146 Cowanodden fault zone, is crosscut by a swarm of Devonian (–Mississippian?) dykes that
1147 intruded contemporaneous sedimentary strata deposited during extensional reactivation of
1148 the eastern portion of the thrust system as a low-angle extensional detachment during late–
1149 post-Caledonian collapse.

1150 4) Timanian thrust systems were overprinted by NNE-dipping, brittle normal faults in the late
1151 Paleozoic during the collapse of the Caledonides and/or subsequent rifting in the Devonian–
1152 Carboniferous.

1153 5) Timanian thrust systems and associated Caledonian and Devonian–Carboniferous brittle
1154 overprints (e.g., Agardhbukta Fault) in the northwestern Norwegian Barents Sea and
1155 Svalbard were mildly reactivated during the early Cenozoic Eurekan tectonic event, which
1156 resulted in minor folding and minor reverse offsets of Devonian–Mesozoic sedimentary
1157 strata and intrusions. Timanian thrusts and related overprints in the northeastern Norwegian
1158 Barents Sea were not reactivated during the Eurekan tectonic event.

1159 6) The presence of hundreds–thousands of kilometers long Timanian thrust systems may
1160 suggest that the Barents Sea and Svalbard’s three basement terranes were already attached
1161 to northern Norway and northwestern Russia in the late Neoproterozoic (ca. 600 Ma). If
1162 correct, a Timanian origin for these structures would preclude any major strike-slip
1163 movements along major N–S-striking faults like the Billefjorden and Lomfjorden fault
1164 zones in the Phanerozoic, and imply that the Caledonian suture zone is located west of or
1165 in western Spitsbergen.

1166

1167 **Acknowledgements**

1168 The present study was supported by the Research Council of Norway, the Tromsø Research
1169 Foundation, and six industry partners through the Research Centre for Arctic Petroleum
1170 Exploration (ARCEX; grant number 228107), the SEAMSTRESS project (grant number 287865),
1171 and the Centre for Earth Evolution and Dynamics (CEED; grant number 223272). We thank the

1172 Norwegian Petroleum Directorate and the Federal Institute for Geosciences and Natural Resources
1173 (BGR) for granting access and allowing publication of seismic, magnetic and gravimetric data in
1174 Svalbard and the Norwegian Barents Sea. Prof. Steffen Bergh, Dr. Winfried Dallmann, Prof. Jiri
1175 Konopasek, Assoc. Prof. Mélanie Forien, Dr. Kate Waghorn (UiT The Arctic University of Norway
1176 in Tromsø), Dr. Peter Klitzke (Federal Institute for Geosciences and Natural Resources –
1177 Germany), Anna Dichiarante (Norway Seismic Array), Rune Matningsdal (Norwegian Petroleum
1178 Directorate), and Prof. Carmen Gaina (Centre for Earth Evolution and Dynamics, University of
1179 Oslo) are thanked for fruitful discussion.

1180

1181 **Data availability**

1182 For high-resolution versions of the figures and supplements, the reader is referred to the
1183 Open Access data repository DataverseNO (doi.org/10.18710/CE8RQH).

1184

1185 **References**

- 1186 Aakvik, R.: Fasies analyse av Undre Karbonske kullførende sedimenter, Billefjorden, Spitsbergen,
1187 Ph.D. Thesis, University of Bergen, Bergen, Norway, 219 pp., 1981.
- 1188 Andresen, A., Haremo, P., Swensson, E. and Bergh, S. G.: Structural geology around the southern
1189 termination of the Lomfjorden Fault Complex, Agardhdalen, east Spitsbergen, Norsk Geol.
1190 Tidsskr., 72, 83–91, 1992.
- 1191 Anell, I., Braathen, A., Olaussen, S. and Osmundsen, P. T.: Evidence of faulting contradicts a
1192 quiescent northern Barents Shelf during the Triassic, *First Break*, 31, 67–76, 2013.
- 1193 Anell, I. M., Braathen, A. and Olaussen, S.: Regional constraints of the Sørkapp Basin: A
1194 Carboniferous relic or a Cretaceous depression, *Mar. Petrol. Geol.*, 54, 123–138, 2014.
- 1195 Anell, I. M., Faleide, J. I. and Braathen, A.: Regional tectono-sedimentary development of the
1196 highs and basins of the northwestern Barents Shelf, *Norsk Geologisk Tidsskrift*, 96, 1, 27–
1197 41, 2016.
- 1198 Arbaret, L. and Burg, J.-P.: Complex flow in lowest crustal, anastomosing mylonites: Strain
1199 gradients in a Kohistan gabbro, northern Pakistan, *J. Geophys. Res.*, 108, 2467, 2003.
- 1200 Barrère, C., Ebbing, J. and Gernigon, L.: Offshore prolongation of Caledonian structures and
1201 basement characterization in the western Barents Sea from geophysical modelling,
1202 *Tectonophys.*, 470, 71–88, 2009.

- 1203 Barrère, C., Ebbing, J. and Gernigon, L.: 3-D density and magnetic crustal characterization of the
1204 southwestern Barents Shelf: implications for the offshore prolongation of the Norwegian
1205 Caledonides, *Geophys. J. Int.*, 184, 1147–1166, 2011.
- 1206 Boyer, S. E. and Elliott, D.: Thrust Systems, *AAPG Bulletin*, 66, 9, 1196–1230, 1982.
- 1207 Braathen, A., Bælum, K., Maher Jr., H. D. and Buckley, S. J.: Growth of extensional faults and
1208 folds during deposition of an evaporite-dominated half-graben basin; the Carboniferous
1209 Billefjorden Trough, Svalbard, *Norsk Geol. Tidsskr.*, 91, 137–160, 2011.
- 1210 Braathen, A., Osmundsen, P. T., Maher, H. and Ganerød, M.: The Keisarhjelmen detachment
1211 records Silurian–Devonian extensional collapse in Northern Svalbard, *Terra Nova*, 30, 34–
1212 39, 2018.
- 1213 Breivik, A. J., Mjelde, R., Grogan, P., Shimamura, H., Murai, Y. and Nishimura, Y.: Caledonide
1214 development offshore–onshore Svalbard based on ocean bottom seismometer, conventional
1215 seismic, and potential field data, *Tectonophys.*, 401, 79–117, 2005.
- 1216 Bro, E. G. and Shvarts, V. H.: Processing results from drill hole Raddedalen-1, Edge Island,
1217 Spitzbergen Archipelago, All-Russian Research Institute for Geology and Mineral
1218 Resources of the World Ocean, St. Petersburg, Pangaea, Report 5750, 1983.
- 1219 Cawood, P. A., McCausland, P. J. A. and Dunning, G. R.: Opening Iapetus: Constraints from the
1220 Laurentian margin in Newfoundland, *GSA Bull.*, 113, 4, 443–453, 2001.
- 1221 Chalmers, J. A. and Pulvertaft, T. C. R.: Development of the continental margins of the Labrador
1222 Sea: a review, in: *Non-Volcanic Rifting of Continental Margins: A Comparison of
1223 Evidence from Land and Sea*, edited by: Wilson, R. C. L., Taylor, R. B. and Froitzheim,
1224 N., *Geol. Soc. London, Spec. Publi.*, 187, 77–105, 2001.
- 1225 Cocks, L. R. M. and Torsvik, T. H.: Baltica from the late Precambrian to mid-Palaeozoic times:
1226 The gain and loss of a terrane’s identity, *Earth-Sci. Rev.*, 72, 39–66, 2005.
- 1227 Colombu, S., Cruciani, G., Fancello, D., Franceschelli, M. and Musumeci, G.: Petrophysical
1228 properties of a granite-protomylonite-ultramylonite sequence: insight from the Monte
1229 Grighini shear zone, central Sardinia, Italy, *Eur. J. Mineral*, 27, 471–486, 2015.
- 1230 Corfu, F., Andersen, T. B. and Gasser, D.: The Scandinavian Caledonides: main features,
1231 conceptual advances and critical questions, in: *New Perspectives on the Caledonides of
1232 Scandinavia and Related Areas*, edited by: Corfu, F., Gasser, D. and Chew, D. M., *Geol.
1233 Soc., London, Spec. Publi.*, 390, 9–43, 2014.

- 1234 Cutbill, J. L. and Challinor, A.: Revision of the Stratigraphical Scheme for the Carboniferous and
 1235 Permian of Spitsbergen and Bjørnøya, *Geol. Mag.*, 102, 418–439, 1965.
- 1236 Cutbill, J. L., Henderson, W. G. and Wright, N. J. R.: The Billefjorden Group (Early Carboniferous)
 1237 of central Spitsbergen, *Norsk Polarinst. Skr.*, 164, 57–89, 1976.
- 1238 Dallmann, W. K.: *Geoscience Atlas of Svalbard*, Norsk Polarinstutt, Tromsø, Norway,
 1239 Rapportserie nr. 148, 2015.
- 1240 Dallmann, W. K. and Krasil'scikov, A. A.: Geological map of Svalbard 1:50,000, sheet D20G
 1241 Bjørnøya, *Norsk Polarinst. Temakart*, 27, 1996.
- 1242 Dallmann, W. K. and Piepjohn, K.: The structure of the Old Red Sandstone and the Svalbardian
 1243 Orogenic Event (Ellesmerian Orogeny) in Svalbard, *Norg. Geol. Unders. B., Spec. Publi.*,
 1244 15, 106 pp., 2020.
- 1245 Dallmeyer, R. D., Peucat, J. J., Hirajima, T. and Ohta, Y.: Tectonothermal chronology within a
 1246 blueschist–eclogite complex, west-central Spitsbergen, Svalbard: Evidence from $^{40}\text{Ar}/^{39}\text{Ar}$
 1247 and Rb–Sr mineral ages, *Lithos*, 24, 291–304, 1990a.
- 1248 Dallmeyer, R. D., Peucat, J. J. and Ohta, Y.: Tectonothermal evolution of contrasting metamorphic
 1249 complexes in northwest Spitsbergen (Biskayerhalvøya): Evidence from $^{40}\text{Ar}/^{39}\text{Ar}$ and Rb-
 1250 Sr mineral ages, *GSA Bull.*, 102, 653–663, 1990b.
- 1251 Dewey, J. F. and Strachan, R. A.: Changing Silurian–Devonian relative plate motion in the
 1252 Caledonides: sinistral transpression to sinistral transtension, *J. Geol. Soc., London*, 160,
 1253 219–229, 2003.
- 1254 Drachev, S. S.: Fold belts and sedimentary basins of the Eurasian Arctic, *Arktos*, 2:21, 2016.
- 1255 Drachev, S. S., Malyshev, N. A. and Nikishin, A. M.: Tectonic history and petroleum geology of
 1256 the Russian Arctic Shelves: an overview, *Petrol. Geol. Conf. series*, 7, 591–619, 2010.
- 1257 Dumais, M.-A. and Brønner, M.: Revisiting Austfonna, Svalbard, with potential field methods – a
 1258 new characterization of the bed topography and its physical properties, *The Cryosphere*,
 1259 14, 183–197, 2020.
- 1260 Eldholm, O. and Ewing, J.: Marine Geophysical Survey in the Southwestern Barents Sea, *J.*
 1261 *Geophys. Res.*, 76, 17, 3832–3841, 1971.
- 1262 Engen, Ø., Faleide, J. I. and Dyreng, T. K.: Opening of the Fram Strait gateway: A review of plate
 1263 tectonic constraints, *Tectonophys.*, 450, 51–69, 2008.

- 1264 Estrada, S., Tessensohn, F. and Sonntag, B.-L.: A Timanian island-arc fragment in North
1265 Greenland: The Midtkap igneous suite, *J. Geodyn.*, 118, 140–153, 2018.
- 1266 Faehnrich, K., Majka, J., Schneider, D., Mazur, S., Manecki, M., Ziemniak, G., Wala, V. T. and
1267 Strauss, J. V.: Geochronological constraints on Caledonian strike-slip displacement in
1268 Svalbard, with implications for the evolution of the Arctic, *Terra Nova*, 2020, 32, 290–299.
- 1269 Fortey, R. A. and Bruton, D. L.: Lower Ordovician trilobites of the Kirtonryggen Formation,
1270 Spitsbergen, *ossils and Strata*, 59, Wiley Blackwell, 120 pp., 2013.
- 1271 Fountain, D. M., Hurich, C. A. and Smithson, S. B.: Seismic relectivity of mylonite zones in the
1272 crust, *Geology*, 12, 195–198, 1984.
- 1273 Friend, P. F. and Moody-Stuart, M.: Sedimentation of the Wood Bay Formation (Devonian) of
1274 Spitsbergen: Regional analysis of a late orogenic basin, *Norsk Polarinst. Skr.*, 157, 80 pp.,
1275 1972.
- 1276 Friend, P. F., Heintz, N. and Moody-Stuart, M.: New unit terms for the Devonian of Spitsbergen
1277 and a new stratigraphical scheme for the Wood Bay Formation, *Polarinst. Årbok*, 1965, 59–
1278 64, 1966.
- 1279 Friend, P. F., Harland, W. B., Rogers, D. A., Snape, I. and Thornley, R. S.: Late Silurian and Early
1280 Devonian stratigraphy and probable strike-slip tectonics in northwestern Spitsbergen, *Geol.*
1281 *Mag.*, 134, 4, 459–479, 1997.
- 1282 Gasser, D.: The Caledonides of Greenland, Svalbard and other Arctic areas: status of research and
1283 open questions, in: *New Perspectives on the Caledonides of Scandinavia and Related Areas*,
1284 edited by: Corfu, F., Gasser, D. and Chew, D. M., *Geol. Soc., London, Spec. Publi.*, 390,
1285 93–129, 2014.
- 1286 Gee, D. G. and Moody-Stuart, M.: The base of the Old Red Sandstone in central north Haakon VII
1287 Land, Vestspitsbergen, *Polarinst. Årbok*, 1964, 57–68, 1966.
- 1288 Gee, D. G. and Pease, V.: The Neoproterozoic Timanide Orogen of eastern Baltica: introduction,
1289 in: *The Neoproterozoic Timanide Orogen of eastern Baltica*, edited by: Gee, D. G. and
1290 Pease, V., *Geol. Soc. London, Mem.*, 30, 1–3, 2004.
- 1291 Gee, D. G. and Teben'kov, A. M.: Svalbard: a fragment of the Laurentian margin, in: *The*
1292 *Neoproterozoic Timanide Orogen of eastern Baltica*, edited by: Gee, D. G. and Pease, V.,
1293 *Geol. Soc. London, Mem.*, 30, 191–206, 2004.

- 1294 Gee, D. G., Björklund, L. and Stølen, L.-K.: Early Proterozoic basement in Ny Friesland–
1295 implications for the Caledonian tectonics of Svalbard, *Tectonophys.*, 231, 171–182, 1994.
- 1296 Gee, D. G., Fossen, H., Henriksen, N. and Higgins, A. K.: From the Early Paleozoic Platforms of
1297 Baltica and Laurentia to the Caledonide Orogen of Scandinavia and Greenland, *Episodes*,
1298 31, 1, 44–51, 2008.
- 1299 Gernigon, L. and Brönnner, M.: Late Palaeozoic architecture and evolution of the southwestern
1300 Barents Sea: insights from a new generation of aeromagnetic data, *J. Geol. Soc., London*,
1301 169, 449–459, 2012.
- 1302 Gernigon, L., Brönnner, M., Roberts, D., Olesen, O., Nasuti, A. and Yamasaki, T.: Crustal and basin
1303 evolution of the southwestern Barents Sea: From Caledonian orogeny to continental
1304 breakup, *Tectonics*, 33, 347–373, 2014.
- 1305 Gernigon, L., Brönnner, M., Dumais, M.-A., Gradmann, S., Grønlie, A., Nasuti, A. and Roberts, D.:
1306 Basement inheritance and salt structures in the SE Barents Sea: Insights from new potential
1307 field data, *J. Geodyn.*, 119, 82–106, 2018.
- 1308 Griffin, W. L., Nikolic, N., O’Reilly, S. Y. and Pearson, N. J.: Coupling, decoupling and
1309 metasomatism: Evolution of crust–mantle relationships beneath NW Spitsbergen, *Lithos*,
1310 149, 115–135, 2012.
- 1311 Gudlaugsson, S. T., Faleide, J. I., Johansen, S. E. and Breivik, A. J.: Late Palaeozoic structural
1312 development of the South-western Barents Sea. *Mar. Petrol. Geol.*, 15, 73–102, 1998.
- 1313 Haremo, P. and Andresen, A.: Tertiary décollements thrusting and inversion structures along
1314 Billefjorden and Lomfjorden Fault Zones, East Central Spitsbergen, in: *Structural and
1315 Tectonic Modelling and its Application to Petroleum Geology*, edited by: Larsen, R. M.,
1316 Brekke, H., Larsen, B. T. and Talleraas, E., Norwegian Petroleum Society (NPF) Special
1317 Publications, 1, 481–494, 1992.
- 1318 Harland, W. B.: Contribution of Spitsbergen to understanding of tectonic evolution of North
1319 Atlantic region, *AAPG Memoirs*, 12, 817–851, 1969.
- 1320 Harland, W. B. and Horsfield, W. T.: West Spitsbergen Orogen, in: *Mesozoic–Cenozoic Orogenic
1321 Belts, data for Orogenic Studies*, *J. Geol. Soc. London, Spec. Publi.*, 4, 747–755, 1974.
- 1322 Harland, W. B. and Kelly, S. R. A.: Eastern Svalbard Platform, in: *Geology of Svalbard*, edited by:
1323 Harland, W. B., *Geol. Soc. London, Mem.*, 17, 521 pp., 1997.

- 1324 Harland, W. B. and Wright, N. J. R.: Alternative hypothesis for the pre-Carboniferous evolution of
1325 Svalbard, Norsk Polarinst. Skr., 167, 89–117, 1979.
- 1326 Harland, W. B., Cutbill, L. J., Friend, P. F., Gobbett, D. J., Holliday, D. W., Maton, P. I., Parker,
1327 J. R. and Wallis, R. H.: The Billefjorden Fault Zone, Spitsbergen – the long history of a
1328 major tectonic lineament, Norsk Polarinst. Skr., 161, 1–72, 1974.
- 1329 Harland, W. B., Scott, R. A., Auckland, K. A. and Snape, I.: The Ny Friesland Orogen, Spitsbergen,
1330 Geol. Mag., 129, 6, 679–708, 1992.
- 1331 Harland, W. B., Hambrey, M. J. and Waddams, P.: Vendian geology of Svalbard, Norsk Polarinst.
1332 Skri., 193, 152 pp., 1993.
- 1333 Hassaan, M.: Evaporite-influenced rift basins and salt tectonics in the southeastern Norwegian
1334 Barents Sea, Ph.D. Thesis, University of Oslo, Oslo, Norway, 305 pp., 2021.
- 1335 Hassaan, M., Faleide, J. I., Gabrielsen, R. H. and Tsikalas, F.: Carboniferous graben structures,
1336 evaporite accumulations and tectonic inversion in the southeastern Norwegian Barents Sea,
1337 Mar. Petrol. Geol., 112, 104038, 2020a.
- 1338 Hassaan, M., Faleide, J. I., Gabrielsen, R. H. and Tsikalas, F.: Architecture of the evaporite
1339 accumulation and salt structures dynamics in Tiddlybanken Basin, southeastern Norwegian
1340 Barents Sea, Basin Res., 33, 91–117, 2020b.
- 1341 Hassaan, M., Faleide, J. I., Gabrielsen, R. H. and Tsikalas, F.: Effects of basement structures and
1342 Carboniferous basin configuration on evaporite distribution and the development of salt
1343 structures in Nordkapp Basin, Barents Sea—Part I, Basin Res., 33, 4, 2474–2499, 2021.
- 1344 Herrevold, T., Gabrielsen, R. H. and Roberts, D.: Structural geology of the southeastern part of the
1345 Trollfjorden-Komagelva Fault Zone, Varanger Peninsula, Finnmark, North Norway,
1346 Norwegian Journal of Geology, 89, 305-325, 2009.
- 1347 Horsfield, W. T.: Glauconite schists of Caledonian age from Spitsbergen, Geol. Mag., 109, 1,
1348 29–36, 1972.
- 1349 Hurich, C. A., Smithson, S. B., Fountain, D. M. and Humphreys, M. C.: Seismic evidence of
1350 mylonite reflectivity and deep structure in the Kettle dome metamorphic core complex,
1351 Washington, Geology, 13, 577–580, 1985.
- 1352 Jakobsson, M., Mayer, L., Coackley, B., Dowdeswell, J. A., Forbes, S., Fridman, B., Hodnesdal,
1353 H., Noormets, R., Pedersen, R., Rebesco, M., Schenke, H. W., Zarayskaya, Y., Accettella,
1354 D., Armstrong, A., Anderson, R. M., Bienhoff, P., Camerlenghi, A., Church, I., Edwards,

1355 M., Gardner, J. V., Hall, J. K., Hell, B., Hestvik, O., Kristoffersen, Y., Marcussen, C.,
 1356 Mohammad, R., Mosher, D., Nghiem, S. V., Pedrosa, M. T., Travaglini, P. G., and
 1357 Weatherall, P.: The International Bathymetric Chart of the Arctic Ocean (IBCAO) Version
 1358 3.0, *Geophys. Res. Lett.*, 39, L12609, <https://doi.org/10.1029/2012GL052219>, 2012.

1359 Johansen, S. E., Ostistoy, B. K., Birkeland, Ø., Fedorovsky, Y. F., Martirosjan, V. N., Bruun
 1360 Christensen, O., Cheredeev, S. I., Ignatenko, E. A. and Margulis, L. S.: Hydrocarbon
 1361 potential in the Barents Sea region: play distribution and potential, in: *Arctic Geology and
 1362 Petroleum Potential*, edited by: Vorren, T. O., Bergsager, E., Dahl-Stammes, Ø. A., Holter,
 1363 E., Johansen, B., Lie, E. and Lund, T. B., *NPF Spec. Publi.*, 2, 273–320, Elsevier,
 1364 Amsterdam, 1992.

1365 Johansson, Å., Larionov, A. N., Gee, D. G., Ohta, Y., Tebenkov, A. M. and Sandelin, S.:
 1366 Grenvillian and Caledonian tectono-magmatic activity in northeasternmost Svalbard, in:
 1367 *The Neoproterozoic Timanide Orogen of Eastern Baltica*, edited by: Gee, D. G. and Pease,
 1368 V., *Geol. Soc. London Memoirs*, 30, 207–232, 2004.

1369 Johansson, Å., Gee, D. G., Larionov, A. N., Ohta, Y. and Tebenkov, A. M.: Grenvillian and
 1370 Caledonian evolution of eastern Svalbard – a tale of two orogenies, *Terra Nova*, 17, 317–
 1371 325, 2005.

1372 Kairanov, B., Escalona, A., Mordascova, A., Sliwinska, K. and Suslova, A.: Early Cretaceous
 1373 tectonostratigraphy evolution of the north central Barents Sea, *J. Geodyn.*, 119, 183–198,
 1374 2018.

1375 Klitzke, P., Franke, D., Ehrhardt, A., Lutz, R., Reinhardt, L., Heyde, I. and Faleide, J. I.: The
 1376 Palaeozoic Evolution of the Olga Basin Region, Northern Barents Sea: A Link to the
 1377 Timanian Orogeny, *Geochem., Geophys., Geosy.*, 20, 614–629, 2019.

1378 Knudsen, C., Gee, D. G., Sherlock, S. C. and Yu, L.: Caledonian metamorphism of metasediments
 1379 from Franz Josef Land, *GFF*, 141, 295–307, 2019.

1380 Koehl, J.-B. P.: Early Cenozoic Eurekan strain partitioning and decoupling in central Spitsbergen,
 1381 Svalbard, *Solid Earth*, 12, 1025–1049, 2020a.

1382 Koehl, J.-B. P.: Impact of Timanian thrusts on the Phanerozoic tectonic history of Svalbard,
 1383 Keynote lecture, EGU General Assembly, May 3rd–8th 2020, Vienna, Austria, 2020b.

1384 Koehl, J.-B. P. and Muñoz-Barrera, J. M.: From widespread Mississippian to localized
 1385 Pennsylvanian extension in central Spitsbergen, Svalbard, *Solid Earth*, 9, 1535–1558, 2018.

- 1386 Koehl, J.-B. P., Bergh, S. G., Henningsen, T. and Faleide, J. I.: Middle to Late Devonian–
1387 Carboniferous collapse basins on the Finnmark Platform and in the southwesternmost
1388 Nordkapp basin, SW Barents Sea, *Solid Earth*, 9, 341–372, 2018.
- 1389 Koehl, J.-B. P., Bergh, S. G., Osmundsen, P. T., Redfield, T., Indrevær, K., Lea, H. and Bergø, E.:
1390 Late Devonian–Carboniferous faulting and controlling structures and fabrics in NW
1391 Finnmark, *Norw. J. Geol.*, 99, 3, 1–40, 2019.
- 1392 Koehl, J.-B. P., Allaart, L. and Noormets, R.: Devonian–Carboniferous collapse and segmentation
1393 of the Billefjorden Trough, and Eurekan inversion–overprint and strain partitioning and
1394 decoupling along inherited WNW–ESE-striking faults, in review, 2021.
- 1395 Korago, E. A., Kovaleva, G. N., Lopatin, B. G. and Orgo, V. V.: The Precambrian rocks of Novaya
1396 Zemlya, in: *The Neoproterozoic Timanide Orogen of Eastern Baltica*, edited by: Gee, D.
1397 G. and Pease, V., *Geol. Soc. London, Mem.*, 30, 135–143, 2004.
- 1398 Kosminska, K., Majka, J., Mazur, S., Krumbholz, M., Klonowska, I., Manecki, M., Czerny, J. and
1399 Dwornik, M.: Blueschist facies metamorphism in Nordenskiöld Land of west-central
1400 Svalbard, *Terra Nova*, 26, 377–386, 2014.
- 1401 Kostyuchenko, A., Sapozhnikov, R., Egorkin, A., Gee, D. G., Berzin, R. and Solodilov, L.: Crustal
1402 structure and tectonic model of northeastern Baltica, based on deep seismic and potential
1403 field data, in: *European Lithosphere Dynamics*, edited by: Gee, D. G. and Stephenson, R.
1404 A., *Geol. Soc. London Mem.*, 32, 521–539, 2006.
- 1405 Labrousse, L., Elvevold, S., Lepvrier, C. and Agard, P.: Structural analysis of high-pressure
1406 metamorphic rocks of Svalbard: Reconstructing the early stages of the Caledonian orogeny,
1407 *Tectonics*, 27, 22 pp., 2008.
- 1408 Lamar, D. L. and Douglass, D. N.: Geology of an area astride the Billefjorden Fault Zone, Northern
1409 Dicksonland, Spitsbergen, Svalbard, *Polarist. Skr.*, 197, 46 pp., 1995.
- 1410 Lamar, D. L., Reed, W. E. and Douglass, D. N.: Billefjorden fault zone, Spitsbergen: Is it part of a
1411 major Late Devonian transform?, *GSA*, 97, 1083–1088, 1986.
- 1412 Larssen, G. B., Elvebakk, G., Henriksen, L. B., Kristensen, S.-E., Nilsson, I., Samuelsberg, T. J.,
1413 Svånå, T. A., Stemmerik, L. and Worsley, D.: Upper Palaeozoic lithostratigraphy of the
1414 Southern part of the Norwegian Barents Sea, *Norges geol. unders. Bull.*, 444, 45 pp., 2005.

- 1415 Lasabuda, A., Laberg, J. S., Knutsen, S.-M. and Safronova, P.: Cenozoic tectonostratigraphy and
1416 pre-glacial erosion: A mass-balance study of the northwestern Barents Sea margin,
1417 Norwegian Arctic, *J. Geodyn.*, 119, 149–166, 2018.
- 1418 Lippard, S. J. and Prestvik, T.: Carboniferous dolerite dykes on Magerøy: new age determination
1419 and tectonic significance, *Norsk Geologisk Tidsskrift*, 77, 159-163, 1997.
- 1420 Livshits, Yu. Ya.: Tectonics of Central Vestspitsbergen, in: *Geology of Spitsbergen*, edited by:
1421 Sokolov, V. N., National Lending Library of Science and Technology, Boston Spa.,
1422 Yorkshire, UK, 59–75, 1965a.
- 1423 Livshits, Yu. Ya.: Paleogene deposits of Nordenskiöld Land, Vestspitsbergen, in: *Geology of*
1424 *Spitsbergen*, edited by: Sokolov, V. N., National Lending Library of Science and
1425 Technology, Boston Spa., Yorkshire, UK, 193–215, 1965b.
- 1426 Lopatin, B. G., Pavlov, L. G., Orgo, V. V. and Shkarubo, S. I.: Tectonic Structure of Novaya
1427 Zemlya, *Polarforschung*, 69, 131–135, 2001.
- 1428 Lorenz, H., Pystin, A. M., Olovyanishnikov, V. G. and Gee, D. G.: Neoproterozoic high-grade
1429 metamorphism of the Kanin Peninsula, Timanide Orogen, northern Russia, in: *The*
1430 *Neoproterozoic Timanide Orogen of Eastern Baltica*, edited by: Gee, D. G. and Pease, V.,
1431 *Geol. Soc. London, Mem.*, 30, 59–68, 2004.
- 1432 Lorenz, H., Männik, P., Gee, D. and Proskurnin, V.: Geology of the Severnaya Zemlya Archipelao
1433 and the North Kara Terrane in the Russian high Arctic, *Int. J. Earth Sci.*, 97, 519–547, 2008.
- 1434 Lowell, J. D.: Spitsbergen tertiary Orogenic Belt and the Spitsbergen Fracture Zone, *GSA Bull.*,
1435 83, 3091–3102, 1972.
- 1436 Lyberis, N. and Manby, G.: Continental collision and lateral escape deformation in the lower and
1437 upper crust: An example from Caledonide Svalbard, *Tectonics*, 18, 1, 40–63, 1999.
- 1438 Majka, J. and Kosminska, K.: Magmatic and metamorphic events recorded within the Southwestern
1439 Basement Province of Svalbard, *Arktos*, 3:5, 2017.
- 1440 Majka, J., Mazur, S., Manecki, M., Czerny, J. and Holm, D. K.: Late Neoproterozoic amphibolite-
1441 facies metamorphism of a pre-Caledonian basement block in southwest Wedel Jarlsberg
1442 Land, Spitsbergen: new evidence from U–Th–Pb dating of monazite, *Geol. Mag.*, 145, 6,
1443 822–830, 2008.

- 1444 Majka, J., Larionov, A. N., Gee, D. G., Czerny, J. and Prsek, J.: Neoproterozoic pegmatite from
1445 Skoddefjellet, Wedel Jarlsberg Land, Spitsbergen: Additional evidence for c. 640 Ma
1446 tectonothermal event in the Caledonides of Svalbard, *Polish Polar Res.*, 33, 1–17, 2012.
- 1447 Majka, J., De'eri-Shlevin, Y., Gee, D. G., Czerny, J., Frei, D. and Ladenberger, A.: Torellian (c.
1448 640 Ma) metamorphic overprint of Tonian (c. 950 Ma) basement in the Caledonides of
1449 southwestern Svalbard, *Geol. Mag.*, 151, 4, 732–748, 2014.
- 1450 Manby, G. M. and Lyberis, N.: Tectonic evolution of the Devonian Basin of northern Spitsbergen,
1451 *Norsk Geol. Tidsskr.*, 72, 7–19, 1992.
- 1452 Manby, G. M., Lyberis, N., Chorowicz, J. and Thiedig, F.: Post-Caledonian tectonics along the
1453 Billefjorden fault zone, Svalbard, and implications for the Arctic region, *Geol. Soc. Am.*
1454 *Bul.*, 105, 201–216, 1994.
- 1455 Manecki, M., Holm, D. K., Czerny, J. and Lux, D.: Thermochronological evidence for late
1456 Proterozoic (Vendian) cooling in southwest Wedel Jarlsberg Land, Spitsbergen, *Geological*
1457 *Magazine*, 135, 63–9, 1998.
- 1458 Marello, L., Ebbing, J. and Gernigon, L.: Magnetic basement study in the Barents Sea from
1459 inversion and forward modelling, *Tectonophys.*, 493, 153–171, 2010.
- 1460 Marello, L., Ebbing, J. and Gernigon, L.: Basement inhomogeneities and crustal setting in the
1461 Barents Sea from a combined 3D gravity and magnetic model, *Geophys. J. Int.*, 193, 2,
1462 557–584, 2013.
- 1463 Mazur, S., Czerny, J., Majka, J., Manecki, M., Holm, D., Smyrak, A. and Wypych, A.: A strike-
1464 slip terrane boundary in Wedel Jarlsberg Land, Svalbard, and its bearing on correlations of
1465 SW Spitsbergen with the Pearya terrane and Timanide belt, *J. Geol. Soc. London*, 166, 529–
1466 544, 2009.
- 1467 McCann, A. J.: Deformation of the Old Red Sandstone of NW Spitsbergen; links to the Ellesmerian
1468 and Caledonian orogenies, in: *New Perspectives on the Old Red Sandstone*, edited by:
1469 Friends, P. F. and Williams, B. P. J., *Geol. Soc. London*, 180, 567–584, 2000.
- 1470 Merdith, A. S., Williams, S. E., Collins, A. S., Tetley, M. G., Mulder, J. A., Blades, M. L., Young,
1471 A., Armistead, S. E., Cannon, J., Zahirovic, S. and Müller, R. D.: Extending full-plate
1472 tectonic models into deep time: Linking the Neoproterozoic and the Phanerozoic, *Earth-*
1473 *Sci. Rev.*, 214, 103477, 2021.

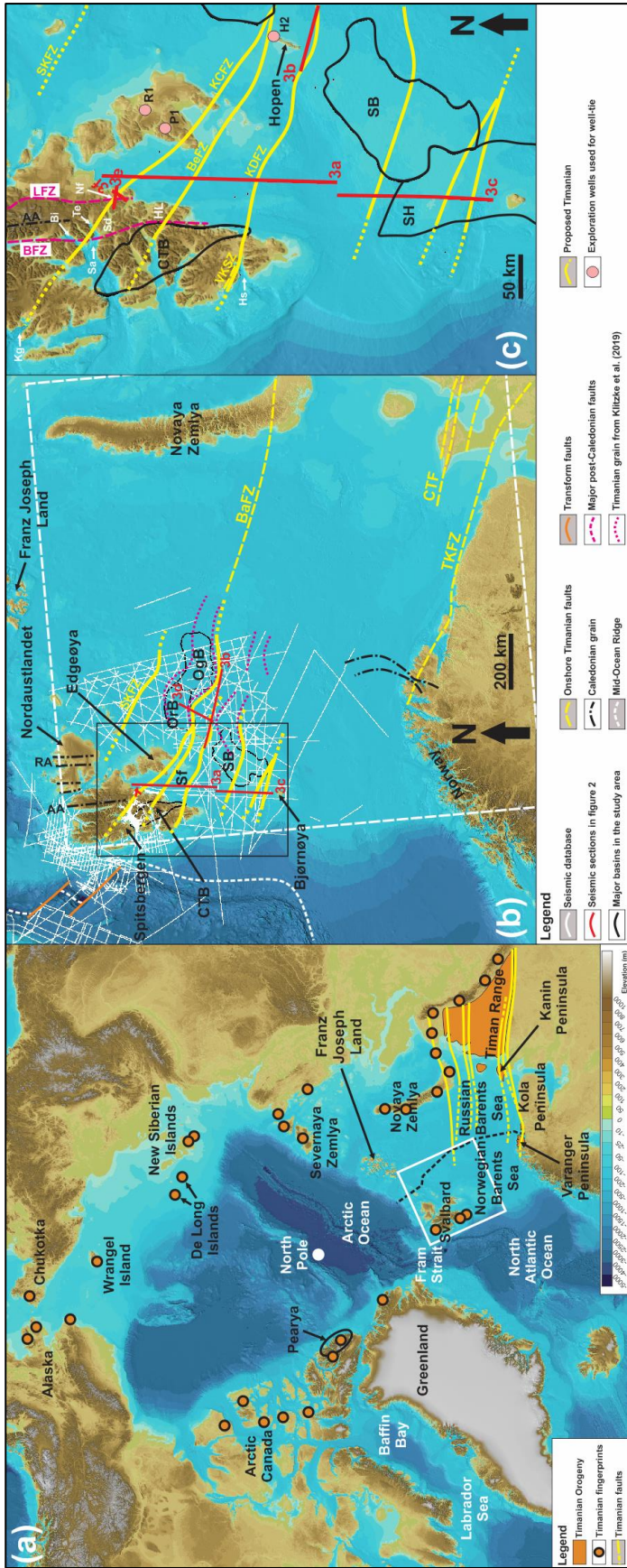
- 1474 Müller, R., Klausen, T. G., Faleide, J. I., Olaussen, S., Eide, C. H. and Suslova, A.: Linking regional
1475 unconformities in the Barents Sea to compression-induced forebulge uplift at the Triassic-
1476 Jurassic transition, *Tectonophys.*, 765, 35–51, 2019.
- 1477 Murascov, L. G. and Mokin, Ju. I.: Stratigraphic subdivision of the Devonian deposits of
1478 Spitsbergen, *Polarinst. Skr.*, 167, 249–261, 1979.
- 1479 Nasuti, A., Roberts, D. and Gernigon, L.: Multiphase mafic dykes in the Caledonides of northern
1480 Finnmark revealed by a new high-resolution aeromagnetic dataset, *Norwegian Journal of*
1481 *Geology*, 95, 251-263, 2015.
- 1482 Norton, M. G., McClay, K. R. and Way, N. A.: Tectonic evolution of Devonian basins in northern
1483 Scotland and southern Norway, *Norsk Geol. Tidsskr.*, 67, 323–338, 1987.
- 1484 Oakey, G. N. and Chalmers, J. A.: A new model for the Paleogene motion of Greenland relative to
1485 North America: Plate reconstructions of the Davis Strait and Nares Strait regions between
1486 Canada and Greenland, *J. of Geophys. Res.*, 117, B10401, 2012.
- 1487 Ogata, K., Mulrooney, M. J., Braathen, A., Maher, H., Osmundsen, P. T., Anell, I., Smyrak-Sikora,
1488 A. A. and Balsamo, F.: Architecture, deformation style and petrophysical properties of
1489 growth fault systems: the Late Triassic deltaic succession of southern Edgeøya (East
1490 Svalbard), *Basin Res.*, 30, 5, 1042–1073, 2018.
- 1491 Ohta, Y., Dallmeyer, R. D. and Peucat, J. J.: Caledonian terranes in Svalbard, *GSA Spec. Paper*,
1492 230, 1–15, 1989.
- 1493 Ohta, Y., Krasil'scikov, A. A., Lepvrier, C. and Teben'kov, A. M.: Northern continuation of
1494 Caledonian high-pressure metamorphic rocks in central-western Spitsbergen, *Polar Res.*,
1495 14, 3, 303–315, 1995.
- 1496 Olovyanishshnikov, V. G., Roberts, D. and Siedlecka, A.: Tectonics and Sedimentation of the
1497 Meso- to Neoproterozoic Timan-Varanger Belt along the Northeastern Margin of Baltica,
1498 *Polarforschung*, 68, 267–274, 2000.
- 1499 Osmundsen, P-T., Braathen, A., Rød, R. S. and Hynne, I. B.: Styles of normal faulting and fault-
1500 controlled sedimentation in the Triassic deposits of Eastern Svalbard, *Norwegian Petroleum*
1501 *directorate Bulletin*, 10, 61–79, 2014.
- 1502 Petersen, T. G., Thomsen, T. B., Olaussen, S. and Stemmerik, L.: Provenance shifts in an evolving
1503 Eurekan foreland basin: the Tertiary Central Basin, Spitsbergen, *J. Geol. Soc., London*, 173,
1504 634–648, 2016.

- 1505 Peucat, J.-J., Ohta, Y., Gee, D. G. and Bernard-Griffiths, J.: U-Pb, Sr and Nd evidence for
1506 Grenvillian and latest Proterozoic tectonothermal activity in the Spitsbergen Caledonides,
1507 Arctic Ocean, *Lithos*, 22, 275–285, 1989.
- 1508 Phillips, T., Jackson, C. A.-L., Bell, R. E., Duffy, O. B. and Fossen, H.: Reactivation of
1509 intrabasement structures during rifting: A case study from offshore southern Norway,
1510 *Journal of Structural Geology*, 91, 54–73, 2016.
- 1511 Piepjohn, K.: The Svalbardian–Ellesmerian deformation of the Old Red Sandstone and the pre-
1512 Devonian basement in NW Spitsbergen (Svalbard), in: *New Perspectives on the Old Red*
1513 *Sandstone*, edited by: Friend, P. F. and Williams, B. P. J., *Geol. Soc. London Spec. Publi.*,
1514 180, 585–601, 2000.
- 1515 Piepjohn, K.: von Gosen, W., Läufer, A., McClelland, W. C. and Estrada, S.: Ellesmerian and
1516 Eurekan fault tectonics at the northern margin of Ellesmere Island (Canadian High Arctic),
1517 *Z. Dt. Ges. Geowiss.*, 164, 1, 81–105, 2013.
- 1518 Piepjohn, K., Dallmann, W. K. and Elvevold, S.: The Lomfjorden Fault Zone in eastern Spitsbergen
1519 (Svalbard), in: *Circum-Arctic Structural Events: Tectonic Evolution of the Arctic Margins*
1520 *and Trans-Arctic Links with Adjacent Orogens*, edited by: Piepjohn, K., Strauss, J. V.,
1521 Reinhardt, L. and McClelland, W. C., *GSA Spec. Paper*, 541, 95–130, 2019.
- 1522 Ramsay, J. G.: Interference Patterns Produced by the Superposition of Folds of Similar Type, *J.*
1523 *Geol.*, 70, 4, 466–481, 1962.
- 1524 Rice, A. H. N.: Restoration of the External Caledonides, Finnmark, North Norway, in: *New*
1525 *Perspectives on the Caledonides of Scandinavia and Related Areas*, Corfu, F., Gasser, D.
1526 and Chew, D. M. (eds), *Geological Society, London, Special Publications*, 390, 271-299,
1527 2014.
- 1528 Roberts, D.: Tectonic Deformation in the Barents Sea Region of Varanger Peninsula, Finnmark,
1529 *Norges geol. unders.*, 282, 1–39, 1972.
- 1530 Roberts, D. and Olovyanishshnikov, V.: Structural and tectonic development of the Timanide
1531 orogeny, in: *The Neoproterozoic Timanide Orogen of Eastern Baltica*, edited by: Gee, D.
1532 G. and Pease, V., *Geol. Soc. London, Mem.*, 30, 47–57, 2004.
- 1533 Roberts, D. and Siedlecka, A.: Timanian orogenic deformation along the northeastern margin of
1534 Baltica, Northwest Russia and Northeast Norway, and Avalonian-Cadomian connections,
1535 *Tectonophysics*, 352, 1r69-184, 2002.

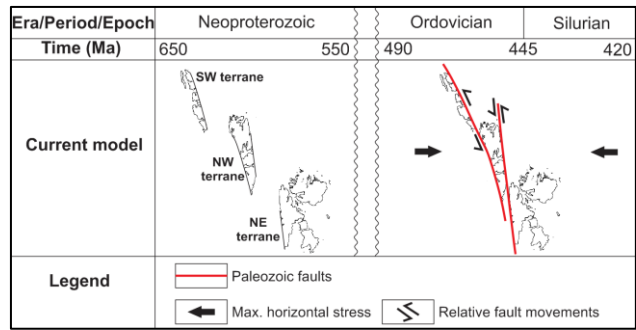
- 1536 Roberts, D. and Williams, G. D.: Berggrunnskart Kjøllefjord 2236 IV, M 1:50.000, foreløpig
1537 utgave, Norges geol. unders., 2013.
- 1538 Roberts, D., Mitchell, J. G. and Andersen, T. B.: A post-Caledonian dyke from Magerøy North
1539 Norway: age and geochemistry, *Norwegian Journal of Geology*, 71, 289-294, 1991.
- 1540 Rosa, D., Majka, J., Thrane, K. and Guarnieri, P.: Evidence for Timanian-age basement rocks in
1541 North Greenland as documented through U–Pb zircon dating of igneous xenoliths from the
1542 Midtkap volcanic centers, *Precambrian Res.*, 275, 394–405, 2016.
- 1543 Schiffer, C., Doré, A. G., Foulger, G. R., Franke, D., Geoffroy, L., Gernigon, L., Holdsworth, B.,
1544 Kuszniir, N., Lundin, E., McCaffrey, K., Peace, A. L., Petersen, K. D., Phillips, T. B.,
1545 Stephenson, R., Stoker, M. S. and Welford, J. K.: Structural inheritance in the North
1546 Atlantic, *Earth-Science Reviews*, 206, 102975, 2020.
- 1547 Senger, K., Roy, S., Braathen, A., Buckley, S., Bælum, K., Gernigon, L., Mjelde, R., Noormets,
1548 R., Ogata, K., Olaussen, S., Planke, S., Ruud, B. O. and Tveranger, J.: Geometries of
1549 doleritic intrusions in central Spitsbergen, Svalbard: an integrated study of an onshore-
1550 offshore magmatic province with applications to CO₂ sequestration, *Norw. J. Geol.*, 93,
1551 143–166, 2013.
- 1552 Siedlecka, A.: Late Precambrian Stratigraphy and Structure of the North-Eastern Margin of the
1553 Fennoscandian Shield (East Finnmark – Timan Region), *Nor. geol. unders.*, 316, 313-348,
1554 1975.
- 1555 Siedlecka, A. and Roberts, D.: Report from a visit to the Komi Branch of the Russian Academy of
1556 Sciences in Syktyvkar, Russia, and from fieldwork in the central Timans, August 1995,
1557 *Norges geol. unders. report*, 95.149, 32 pp., 1995.
- 1558 Siedlecka, A. and Siedlecki, S.: Some new aspects of the geology of Varanger peninsula (Northern
1559 Norway), *Nor. geol. unders.*, 247, 288-306, 1967.
- 1560 Siedlecka, A. and Siedlecki, S.: Late Precambrian sedimentary rocks of the Tanafjord–
1561 Varangerfjord region of Varanger Peninsula, Northern Norway, in: *The Caledonian
1562 Geology of Northern Norway*, edited by: Roberts, D. and Gustavson, M., *Norges geol.
1563 unders.*, 269, 246–294, 1971.
- 1564 [Smelror, M., Petrov, O. V., Larssen, G. B. and Werner, S. C.: Geological Atlas of the Barents Sea,
1565 Geological Survey of Norway, Trondheim, Norway, 2009.](#)

- 1566 Smyrak-Sikora, A., Osmundsen, P. T., Braathen, A., Ogata, K., Anell, I., Mulrooney, M. J. and
1567 Zuchuat, V.: Architecture of growth basins in a tidally influenced, prodelta to delta-front
1568 setting: The Triassic succession of Kvalpynten, East Svalbard, *Basin Research*, 32, 5, 959–
1569 988, 2020.
- 1570 Stouge, S., Christiansen, J. L. and Holmer, L. E.: Lower Palaeozoic stratigraphy of
1571 Murchisonfjorden and Sparreneset, Nordaustlandet, Svalbard, *Geografiska Annaler: Series*
1572 *A, Physical Geography*, 93, 209–226, 2011.
- 1573 Sturt, B. A., Pringle, I. R. and Ramsay, D. M.: The Finnmarkian phase of the Caledonian Orogeny,
1574 *J. Geol., Soc., London*, 135, 597–610, 1978.
- 1575 Thiede, J., Pfirman, S., Schenke, H.-W. and Reil, W.: Bathymetry of Molloy Deep: Fram Strait
1576 Between Svalbard and Greenland, *Mar. Geophys. Res.*, 12, 197–214, 1990.
- 1577 Tonstad, S. A.: The Late Paleozoic development of the Ottar basin from seismic 3D interpretation,
1578 Master's Thesis, University of Tromsø, Tromsø, Norway, 135 pp., 2018.
- 1579 Torsvik, T. H. and Trench, A.: The Ordovician history of the Iapetus Ocean in Britain: new
1580 palaeomagnetic constraints, *J. Geol. Soc., London*, 148, 423–425, 1991.
- 1581 Torsvik, T. H., Burke, K., Steinberger, B., Webb, S. J. and Ashwal, L. D.: Diamond sampled by
1582 plumes from the core–mantle boundary, *Nature Lett.*, 466, 352–355, 2010.
- 1583 Townsend, C.: Thrust transport directions and thrust sheet restoration in the Caledonides of
1584 Finnmark, North Norway, *J. Structural Geol.*, 9, 3, 345–352, 1987.
- 1585 Vernikovsky, V. A., Metelkin, D. V., Vernikovskaya, A. E., Matushkin, N. Yu., Lobkovsky, L. I.
1586 and Shipilov, E. V.: Early evolution stage of the arctic margins (Neoproterozoic-Paleozoic)
1587 and plate reconstructions, *ICAM VI Proceedings*, May 2011, Fairbanks, Alaska, USA, 265–
1588 285, 2011.
- 1589 Von Gosen, W. and Piepjohn, K.: Polyphase Deformation in the Eastern Hornsund Area, *Geol. Jb.*,
1590 B91, 291–312, 2001.
- 1591 Witt-Nilsson, P., Gee, D. G. and Hellman, F. J.: Tectonostratigraphy of the Caledonian Atomfjella
1592 Antiform of northern Ny Friesland, Svalbard, *Norsk Geol. Tidsskr.*, 78, 67–80, 1998.
- 1593 Worsley, D., Agdestein, T., Gjelberg, J. G., Kirkemo, K., Mørk, A., Nilsson, I., Olaussen, S., Steel,
1594 R. J. and Stemmerik, L.: The geological evolution of Bjørnøya, Arctic Norway:
1595 implications for the Barents Shelf, *Norsk Geol. Tidsskr.*, 81, 195–234, 2001.

1596 Ziegler, P. A.: Evolution of the Arctic–North Atlantic and the Western Tethys, AAPG Mem. 43,
1597 1988.
1598

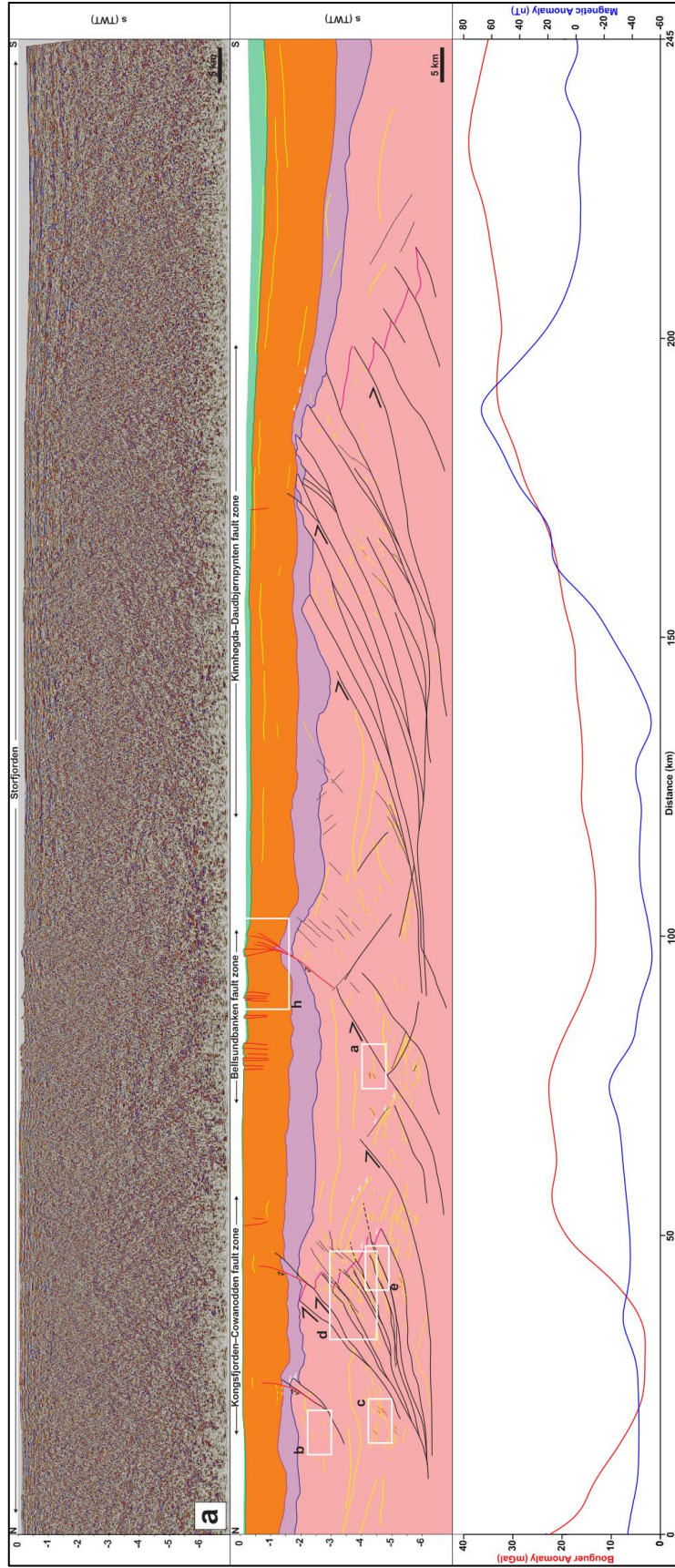


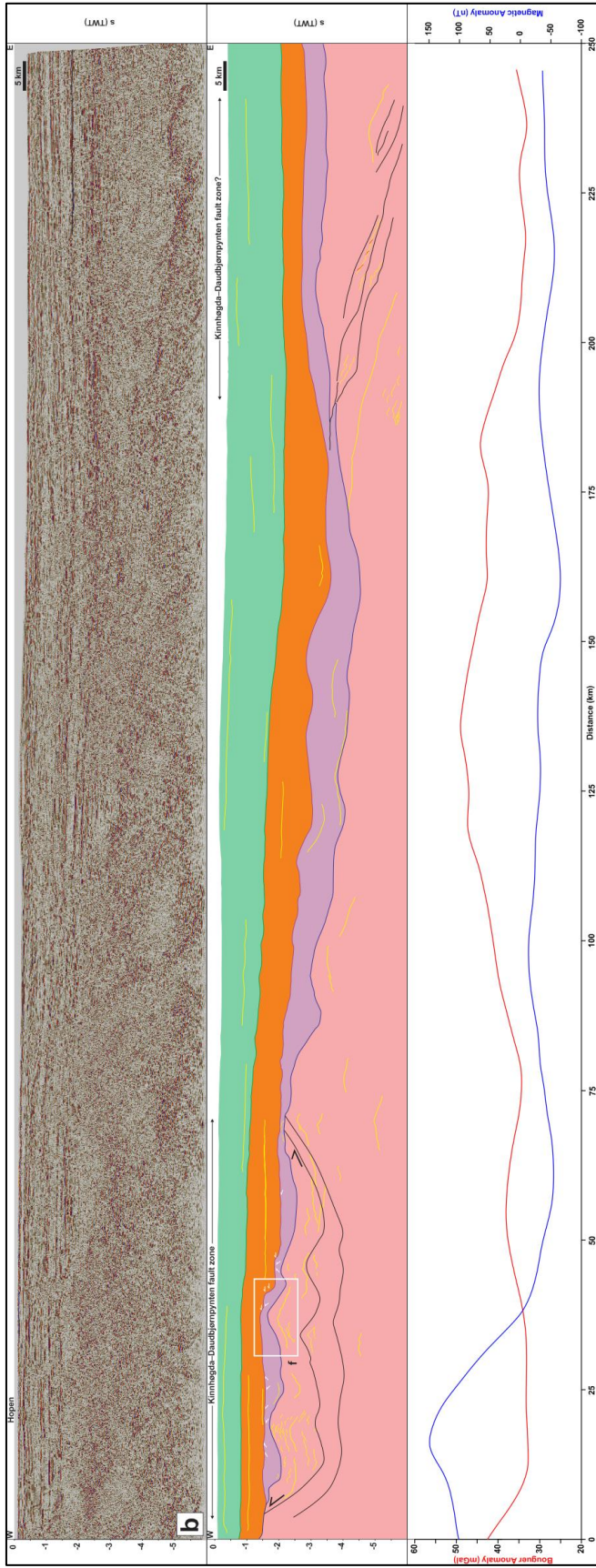
1601 **Figure 1: (a) Overview map showing the Timanian belt in Russia and Norway, and occurrences of Timanian fingerprints**
1602 **throughout the Arctic; (b) Regional map of Svalbard and the Barents Sea the main geological elements and the seismic**
1603 **database used in the present study. The location of (b) is shown as a white frame in (a); (c) Zoom in the northern Norwegian**
1604 **Barents Sea and Svalbard showing the main faults and basins in the study area, and the proposed Timanian structures. The**
1605 **location of (c) is shown as a black frame in (b). The location of the Raddedalen-1 well is from Smyrak-Sikora et al. (2020).**
1606 **Topography and bathymetry are from Jakobsson et al. (2012). Abbreviations: AA: Atomfjella Antiform; BaFZ: Baidaratsky**
1607 **fault zone; BeFZ: Bellsundbanken fault zone; BFZ: Billefjorden Fault Zone; Bi: Billefjorden; CTB: Central Tertiary Basin;**
1608 **HL: Heer Land; Hs: Hornsund; H2: Hopen-2; KCFZ: Kongsfjorden–Cowanodden fault zone; KDFZ: Kinnhøgda–**
1609 **Daudbjørnpynten fault zone; Kg: Kongsfjorden; LFZ: Lomfjorden Fault Zone; Nf: Nordmannsfonna; OgB: Olga Basin;**
1610 **OrB: Ora Basin; P1: Plurdalen-1; RA: Rijpdalen Anticline; R1: Raddedalen-1; Sa: Sassenfjorden; SB: Sørkapp Basin; Sf:**
1611 **Storfjorden; SH: Stappen High; SKFZ: Steiløya–Krylen fault zone; Te: Tempelfjorden; TKFZ: Trollfjorden–Komagelva**
1612 **Fault Zone; VKSZ: Vimsodden–Kosibapasset Shear Zone.**

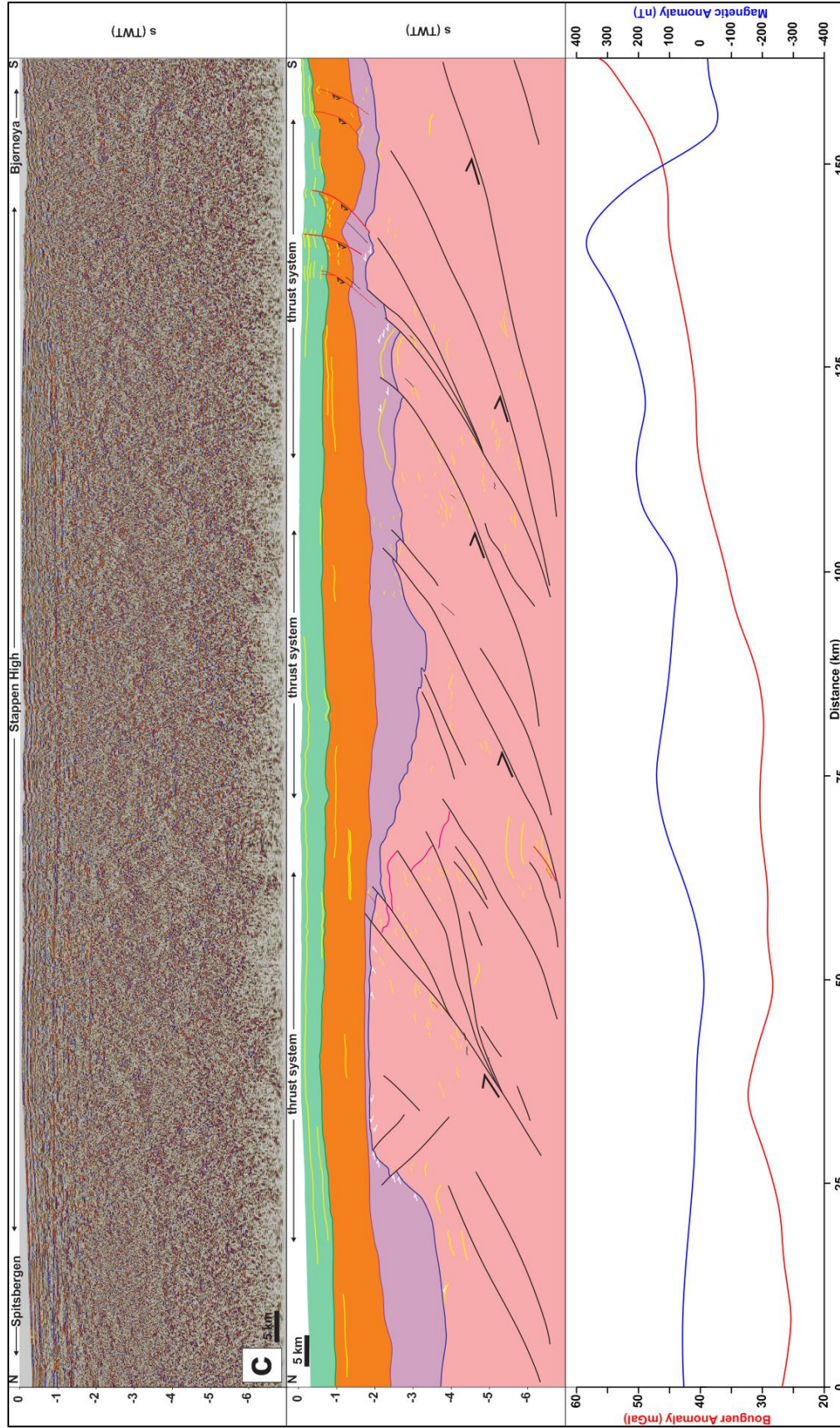


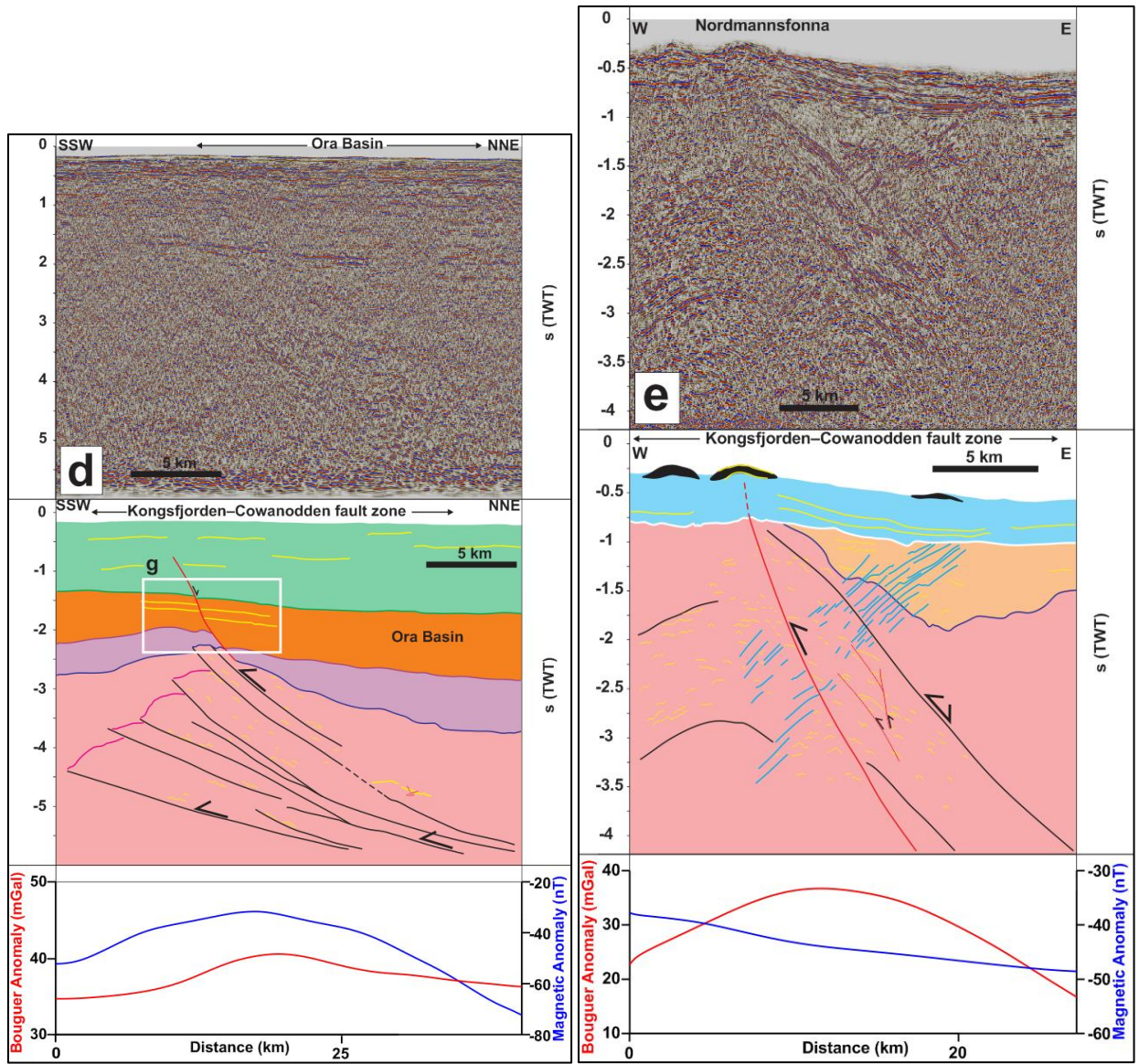
1613

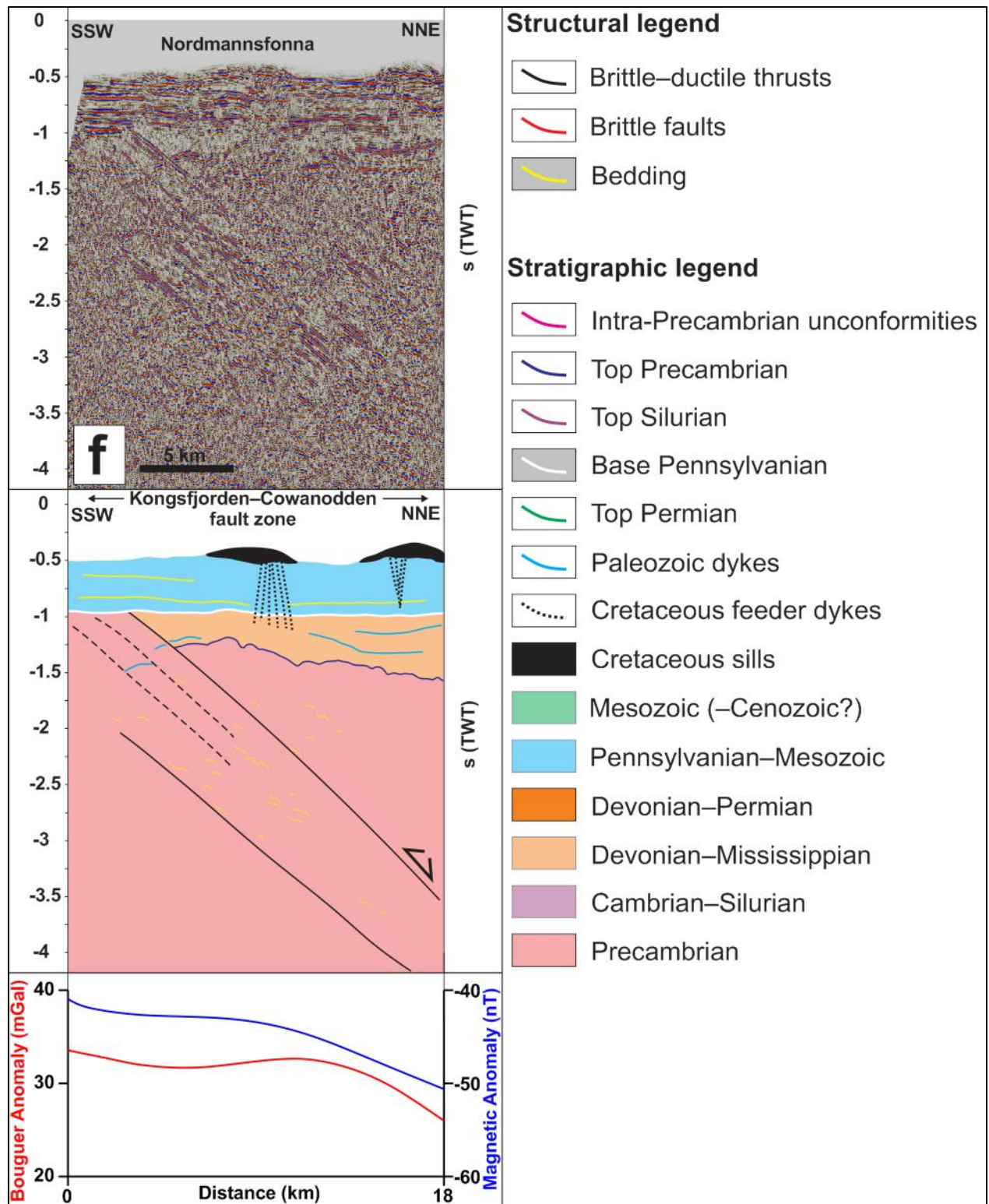
1614 **Figure 2: Paleogeographic reconstruction of the Svalbard Archipelago in the latest Neoproterozoic during the Timanian**
 1615 **Orogeny and in the early–mid Paleozoic during the Caledonian Orogeny according to previous models (e.g., Harland, 1969;**
 1616 **Labrousse et al., 2008).**









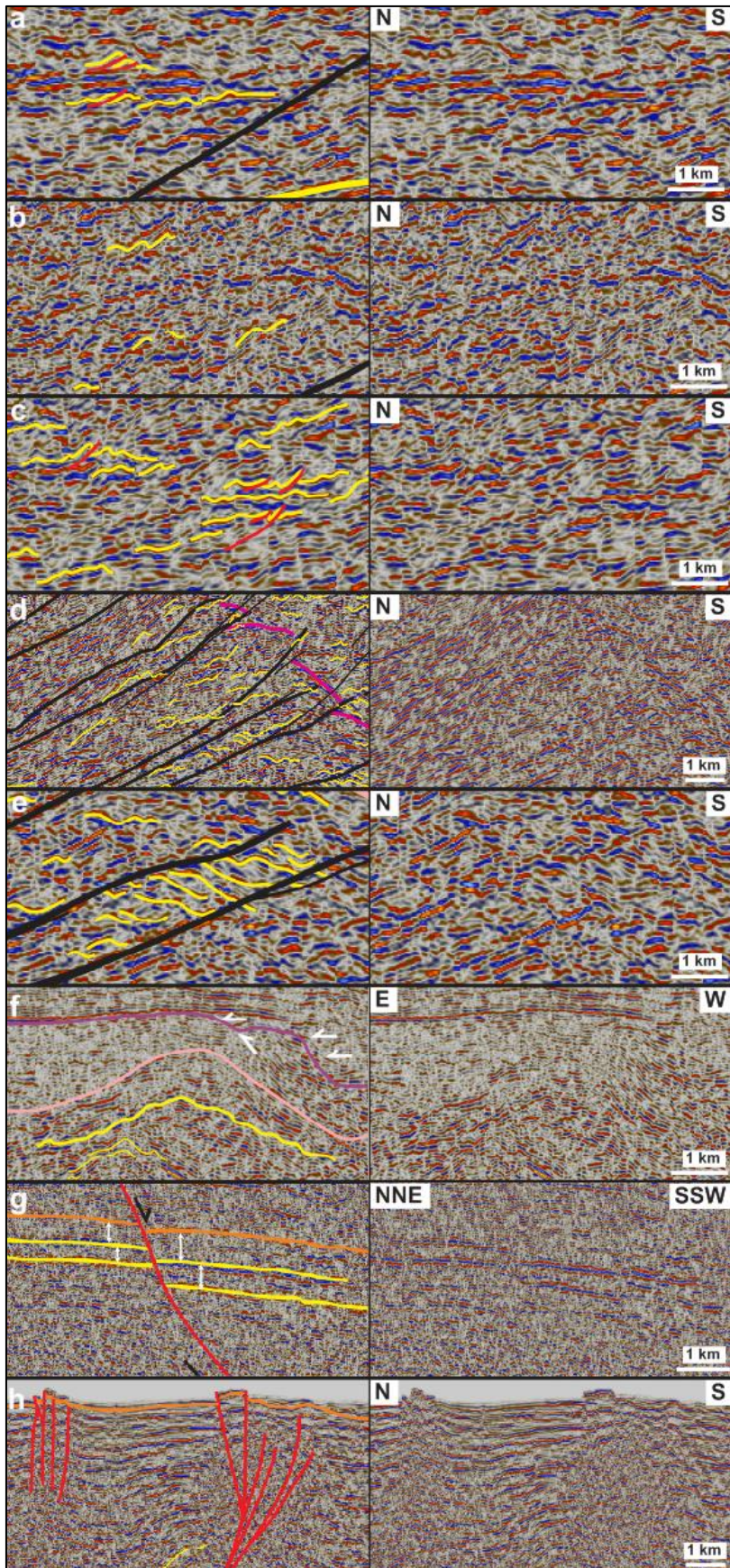


1621

1622 Figure 3: Interpreted seismic profiles and associated potential field data (a) in Storfjorden, (b) south of Hopen, (c) on the
 1623 Stappen High in the northwestern Norwegian Barents Sea between Spitsbergen and Bjørnøya, (d) on the southern flank of
 1624 the Ora Basin in the northeastern Norwegian Barents Sea, and (e and f) in Nordmannsfonna in eastern Spitsbergen. The
 1625 seismic profiles show top-SSW Timanian thrusts that were reactivated and overprinted during subsequent tectonic events
 1626 such as Caledonian contraction, Devonian-Carboniferous late-post Caledonian collapse and rifting, Eurekan contraction,
 1627 and present-day contraction. Profiles (e) and (f) also show Paleozoic and Cretaceous intrusions. The white frames show the

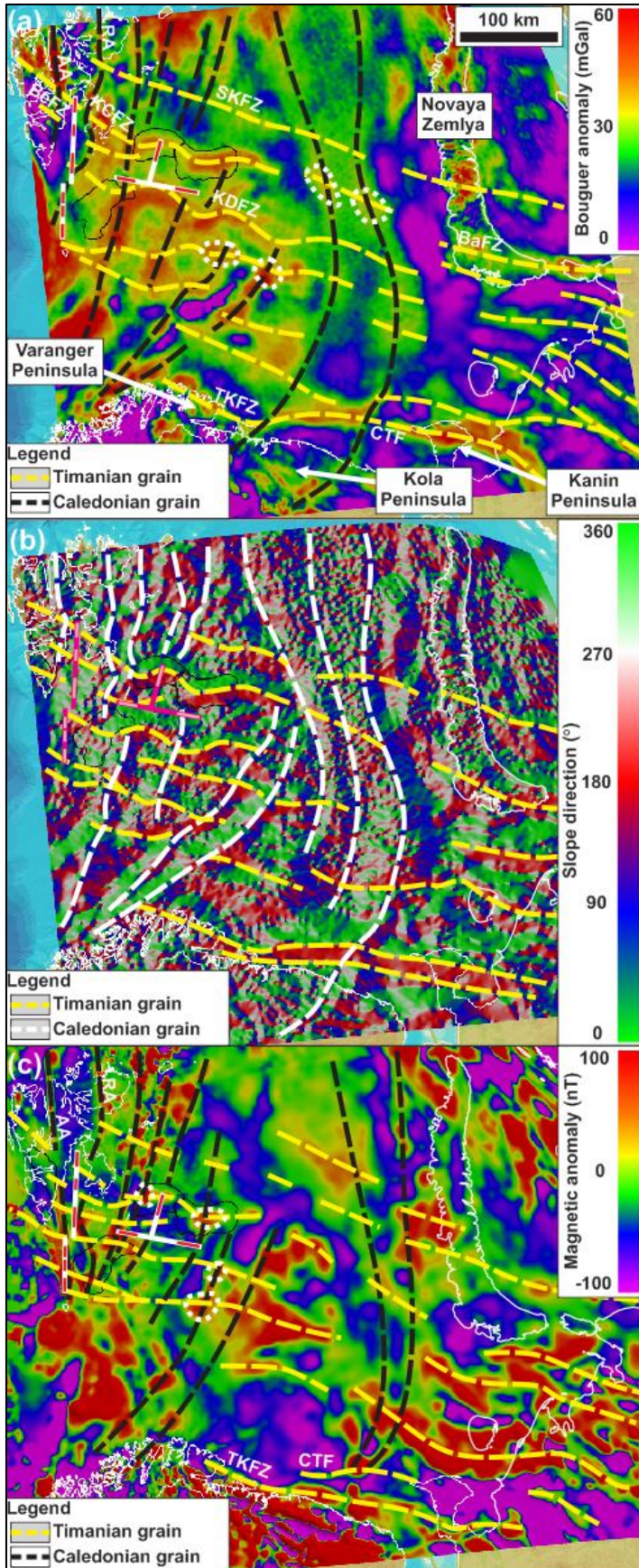
1628 location of zoomed-in portions of the profiles displayed in [Figure 4](#). Potential field data below the seismic profiles
1629 include Bouguer anomaly (red lines) and magnetic anomaly (blue lines). The potential field data show consistently high
1630 gravimetric anomalies and partial correlation with high magnetism towards the footwall of each major thrust systems (i.e.,
1631 towards thickened portions of the crust).

1632



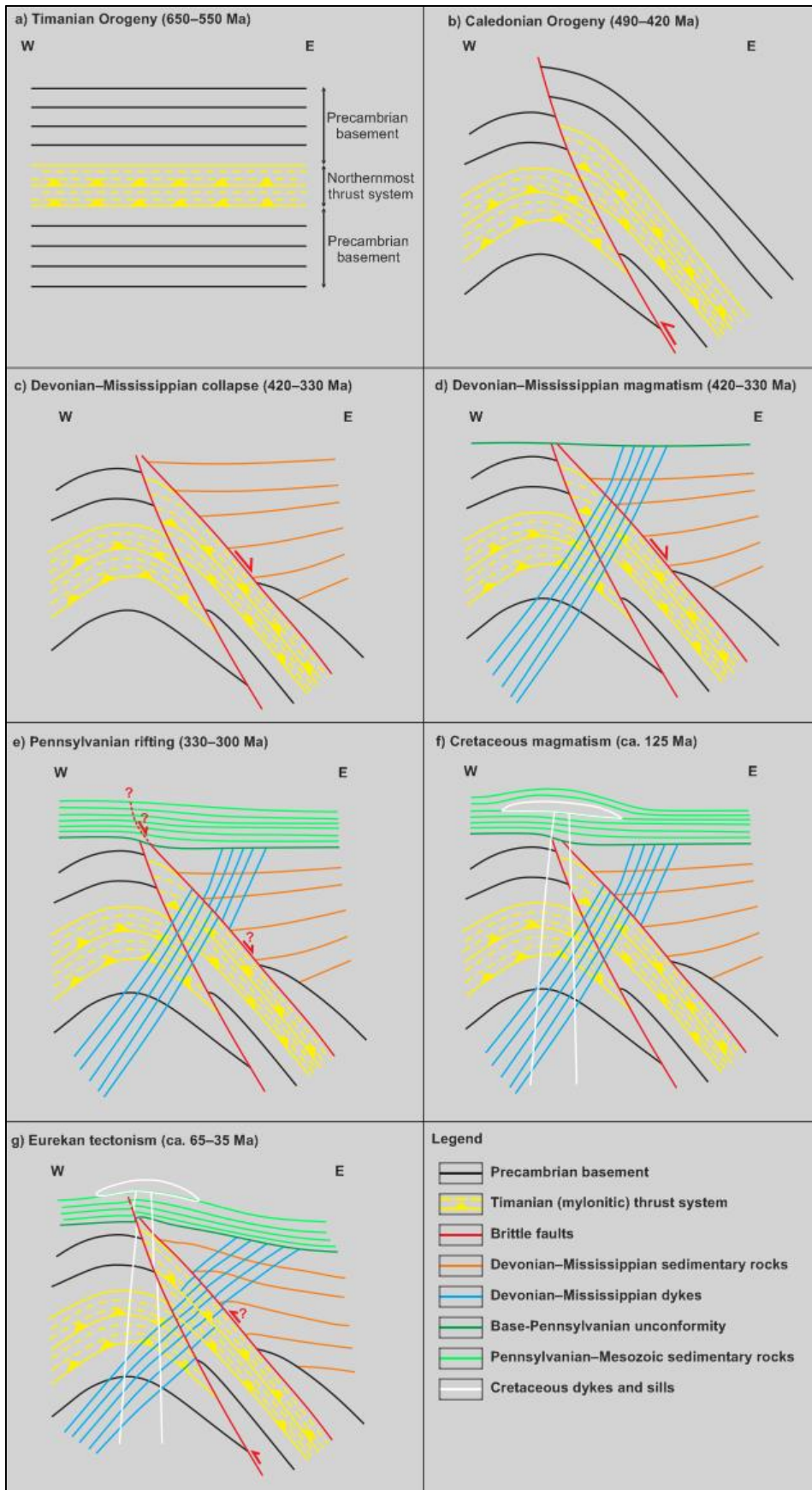
1634 Figure 4: Zooms in seismic profiles shown in [Figure 3](#) showing (a) upright fold structures, (b) SSW-verging folds
1635 and (c) top-SSW minor thrusts in Precambrian–lower Paleozoic (meta-) sedimentary basement rocks, (d) SSW-verging folds
1636 and NNE-dipping mylonitic shear zones within a major thrust that offsets major basement unconformities (fuchsia lines)
1637 top-SSW, (e) duplex structures within a major top-SSW thrust, (f) a N–S- to NNE–SSW-trending, 5–15 kilometers wide,
1638 symmetrical, upright macro-fold and associated, kilometer- to hundreds of meter-scale, parasitic macro- to meso-folds, (g)
1639 syn-tectonic thickening in Devonian–Carboniferous (–Permian?) sedimentary strata offset down-NNE by a normal fault
1640 that merges with a thick mylonitic shear zone at depth, and (h) recent–ongoing reverse offsets of the seafloor reflection by
1641 multiple, inverted, NNE-dipping normal faults in Storfjorden. See [Figure 3](#) for location of each zoom and for legend.

1642



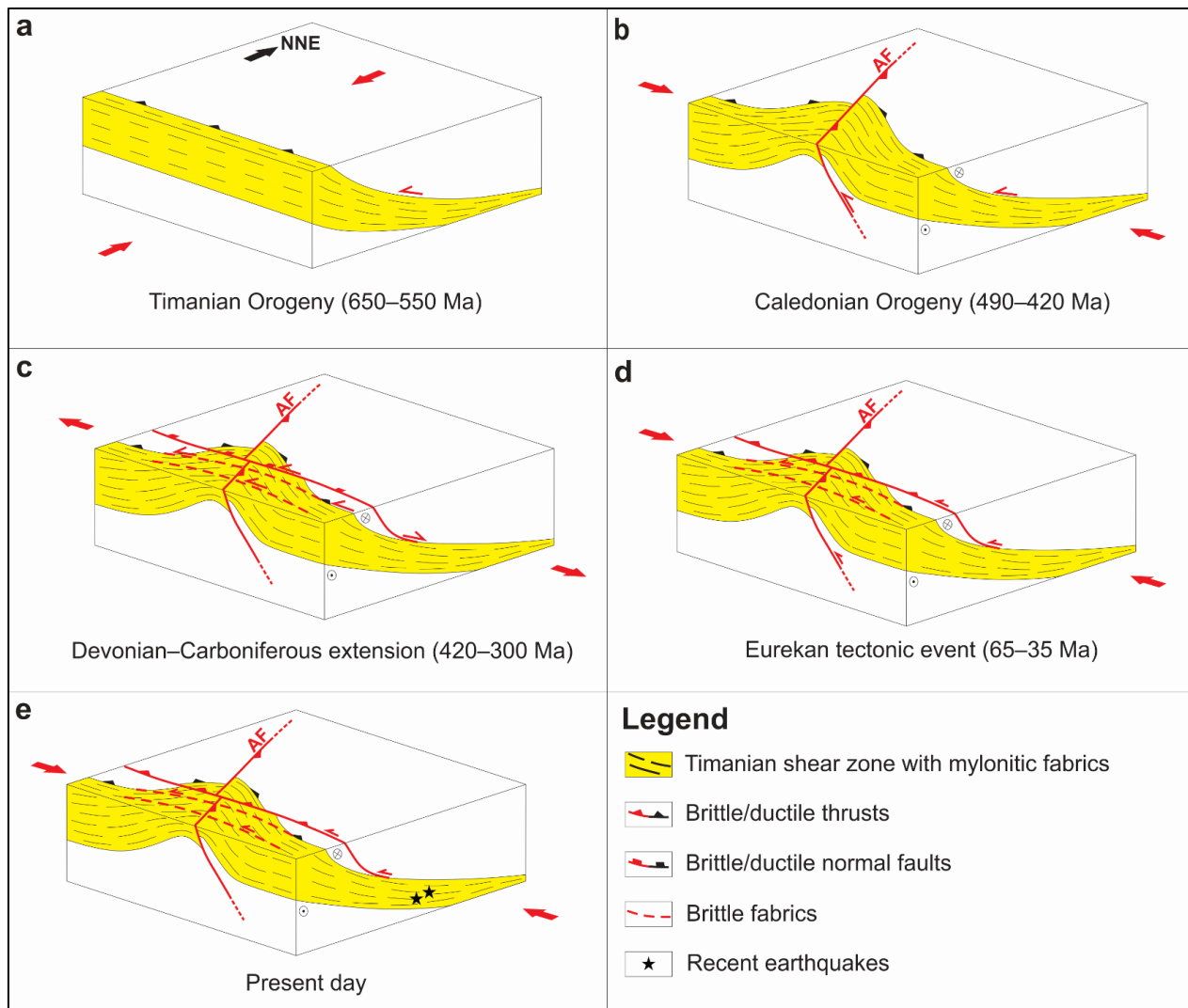
1644 **Figure 5: Gravimetric (a and b) and magnetic (c) anomaly maps over the Barents Sea and adjacent onshore areas in Russia**
1645 **(see location as a dashed white frame in [Figure 1](#)[Figure 1b](#)), Norway and Svalbard showing E–W- to NW–SE-trending**
1646 **anomalies (dashed yellow lines) that correlate with the proposed NNE-dipping Timanian thrust systems in Svalbard and the**
1647 **northern Norwegian Barents Sea. Note the high obliquity of E–W- to NW–SE-trending Timanian grain with NE–SW- to N–**
1648 **S-trending Caledonian grain (dashed black/white lines). Note that dashed lines in (a) and (c) denote high gravimetric and**
1649 **magnetic anomalies. Also notice the oval-shaped high gravimetric and magnetic anomalies (dotted white lines) at the**
1650 **intersection of WNW–ESE- and N–S- to NNE–SSW-trending anomalies in (a) and (c) resulting from the interaction of the**
1651 **two (Timanian and Caledonian) thrust and fold trends. The location of seismic profiles presented in [Figure 3](#)[Figure 3a–d](#)**
1652 **are shown as thick white lines in (a) and (c) and as fuchsia lines in (b). Within these thick white and fuchsia lines, the location**
1653 **and extent of thrust systems evidenced on seismic data ([Figure 3](#)[Figure 3](#)) is shown in white in (a) and (c) and in pink in (b).**
1654 **For the E–W-trending seismic profile shown in [Figure 3](#)[Figure 3b](#), this implies that the red and pink lines represent N–S-**
1655 **trending synclines. Abbreviations: AA: Atomfjella Antiform; BaFZ: Baidaratsky fault zone; BeFZ: Bellsundbanken fault**
1656 **zone; CTF: Central Timan Fault; KCFZ: Kongsfjorden–Cowanodden fault zone; KDFZ: Kinnhøgda–Daudbjørnpynten**
1657 **fault zone; RA: Rijpdalen Anticline; SKFZ: Steiløya–Krylen fault zone; TKFZ: Trollfjorden–Komagelva Fault Zone.**

1658



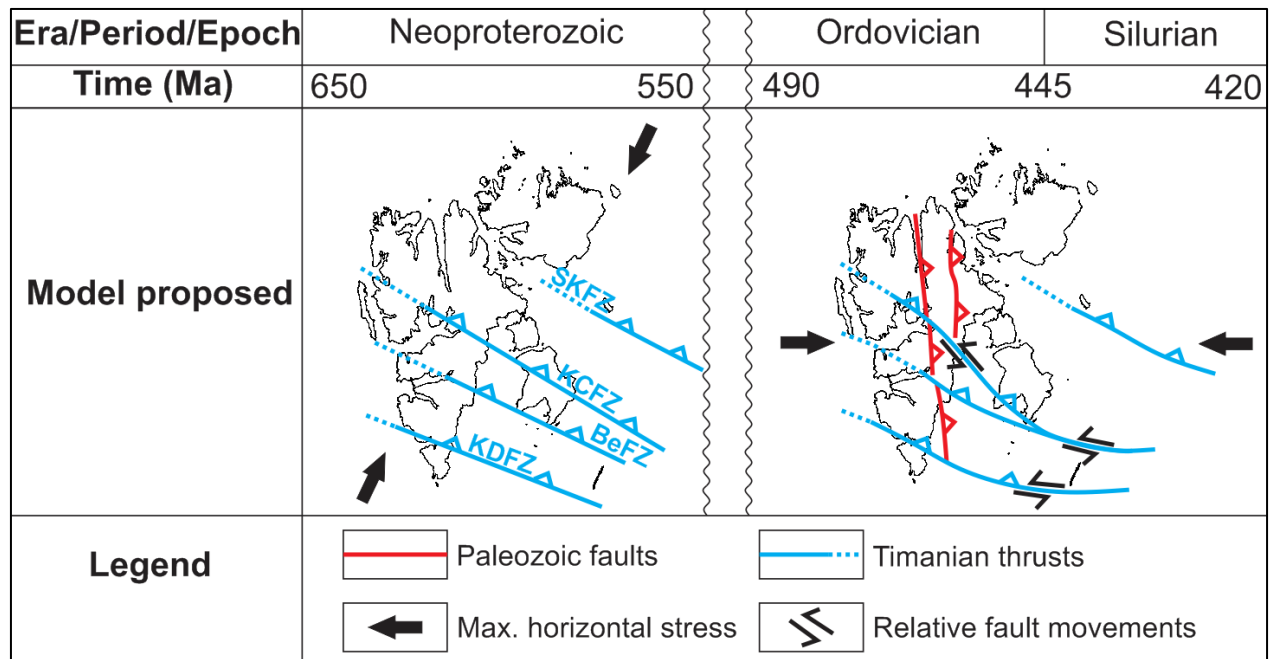
1660 **Figure 6: Sketches showing a possible reconstruction of the tectonic history of the E–W seismic profile in Nordmannsonna**
1661 **shown in [Figure 3](#) ~~Figure 3~~e. (a) Formation of a NNE-dipping, mylonitic thrust system (Kongsfjorden–Cowanodden fault**
1662 **zone) within Precambrian basement rocks during the Timanian Orogeny in the latest Neoproterozoic. The NNE-dipping**
1663 **Kongsfjorden–Cowanodden fault zone appears near horizontal on the E–W transect; (b) Top-west thrusting along the east-**
1664 **dipping Agardhbukta Fault and folding of the Kongsfjorden–Cowanodden fault zone into a broad, moderately NNE-**
1665 **plunging anticline during the Caledonian Orogeny; (c) Inversion of the Kongsfjorden–Cowanodden fault zone along the**
1666 **eastern flank of the Caledonian anticline and deposition of thickened, gently west-dipping, syn-tectonic, Devonian (–**
1667 **Mississippian?) sedimentary strata during post-Caledonian collapse-related extension; (d) Intrusion of Precambrian**
1668 **basement and Devonian (–Mississippian?) sedimentary rocks by steeply west-dipping dykes in the Devonian–Mississippian;**
1669 **(e) Regional erosion in the mid-Carboniferous (latest Mississippian) and deposition of Pennsylvanian sedimentary strata,**
1670 **possibly along a high-angle brittle splay of the inverted portion of the Kongsfjorden–Cowanodden fault zone during rift-**
1671 **related extension; (f) Deposition of Mesozoic sedimentary strata and intrusion of Cretaceous dolerite dykes and sills; (g)**
1672 **Erosion of Pennsylvanian–Mesozoic strata and reactivation of the Kongsfjorden–Cowanodden fault zone and Agardhbukta**
1673 **Fault with minor reverse movements in the early Cenozoic during the Eurekan tectonic event as shown by mild folding and**
1674 **offset of overlying post-Caledonian sedimentary strata, dykes and Base-Pennsylvanian unconformity. Also note the back-**
1675 **tilting (i.e., clockwise rotation) of Devonian–Mississippian dykes in the hanging wall of the Agardhbukta Fault and of the**
1676 **Kongsfjorden–Cowanodden fault zone.**

1677



1678
 1679 **Figure 7: Tectonic evolution of Timanian thrust systems in eastern Spitsbergen, Storfjorden and the northwestern**
 1680 **Norwegian Barents Sea including (a) top-SSW thrusting during the Timanian Orogeny, (b) reactivation as oblique-slip**
 1681 **sinistral-reverse thrusts and offset by top-west brittle thrust overprints (e.g., Agardhbukta Fault – AF) under E–W**
 1682 **contraction during the Caledonian Orogeny, (c) reactivation as low-angle, brittle–ductile, normal–sinistral extensional**
 1683 **detachments and overprinting by high-angle normal–sinistral brittle faults during Devonian–Carboniferous, late–post-**
 1684 **Caledonian extensional collapse and rifting, (d) reactivation as brittle–ductile sinistral–reverse thrusts, overprinting by**
 1685 **high-angle sinistral–reverse brittle thrusts, and mild offset by reactivated top-west thrusts (e.g., Agardhbukta Fault – AF)**
 1686 **during E–W Eurekan contraction, and (e) renewed, recent–ongoing, sinistral–reverse reactivation and overprinting possibly**
 1687 **due to ongoing magma extrusion and transform faulting (ridge-push?) in the Fram Strait.**

1688



1689

1690 **Figure 8: Paleogeographic reconstruction of the Svalbard Archipelago in the latest Neoproterozoic during the Timanian**
 1691 **Orogeny and in the early–mid Paleozoic during the Caledonian Orogeny according to the present study.**